PETROLEUM QUALITY ANALYSIS WITHIN THE UTICA-POINT PLEASANT PLAY OF OHIO, UNITED STATES

by

Richard Boakye Yiadom

A thesis submitted to the faculty of
The University of Utah
in partial fulfillment of the requirements for the degree of

Master of Science

in

Petroleum Engineering

Department of Chemical Engineering

The University of Utah

August 2017

The University of Utah Graduate School

STATEMENT OF THESIS APPROVAL

The thesis of **Richard Boakye Yiadom**

has been approved by the following supervisory committee members:

Milind Deo	, Chair	**4/18/2017** Date Approved
David Thul	, Member	**4/18/2017** Date Approved
John McLennan	, Member	**4/17/2017** Date Approved

and by **Milind Deo** , Chair/Dean of

the Department/College/School of **Chemical Engineering**

and by David B. Kieda, Dean of The Graduate School.

ABSTRACT

The Ordovician age Utica-Point Pleasant (UPP) formation found in eastern Ohio has demonstrated, over the past 7 years through production, to be a significant shale play in the United States. Historical production data show that the play is predominantly gas producing. Conversely, and although relatively minimal production compared to gas, oil production zones do exist, and trend from the northwestern towards the central part of Ohio. In recent years, the UPP formation has received substantial industry attention because of its projected production potential. However, due to limited exploration outside the gas window and little understanding of the maturity levels within the formation, the production potential for unconventional oil remains uncertain in the UPP play.

Using a newly developed pyrolysis method, Incremental S1 (IS1), on a suite of samples from four wells located in zones of low maturity, oil maturity, and condensate maturity, oil quality can be predicted. To complement and validate the newly developed IS1 method for determining oil quality, selected UPP samples were also sent to GeoMark Research to perform oil extraction and gas chromatography analysis. Combining GC extraction and IS1 results, petroleum quality within the Utica-Point Pleasant formation of Ohio can be better resolved, facilitating the potential for production within the play.

TABLE OF CONTENTS

LIST OF TABLES

Tables

NOMENCLATURE

IS1 – Incremental S1

FID – Flame Ionization Detector

UPP – Utica-Point Pleasant

ODNR – Ohio Department of Natural Resources

S1 – Free Petroleum Content (mg of HC/g of rock)

S1_1 – Free Petroleum Released at 50°C (mg of HC/g of rock)

S1_2 – Free Petroleum Released at 100°C (mg of HC/g of rock)

S1_3 – Free Petroleum Released at 150°C (mg of HC/g of rock)

S1_4 – Free Petroleum Released at 200°C (mg of HC/g of rock)

S1_5 – Free Petroleum Released at 250°C (mg of HC/g of rock)

S1_6 – Free Petroleum Released at 300°C (mg of HC/g of rock)

S2 – Kerogen Content (mg of HC/g of rock)

S3 – Carbon Dioxide and Carbon Monoxide Released during Pyrolysis (mg of CO2 or CO/g of rock)

Sl – Light Petroleum Fraction Released at 50°C - 100°C

Sm – Medium Petroleum Fraction Released at 150°C - 200°C

Sh – Heavy Petroleum Fraction Released at 250°C - 300°C

C15-C21 – Light Petroleum (GC Extract)

C22-C28 – Medium Petroleum (GC Extract)

C29-C35 – Heavy Petroleum (GC Extract)

Tmax – Maximum Temperature of S2 Release (°C)

TOC – Total Organic Carbon (%)

API – American Petroleum Institute

GC – Gas Chromatography

IR – Infrared

PQA – Petroleum Quality Analysis

ACKNOWLEDGEMENTS

I would like to, first and foremost, sincerely thank the Almighty Father for giving me the opportunity to complete this research and this phase of my academic career. My profound gratitude to my primary supervisor, David J. Thul, for his unwavering support, both financially and technically, throughout this research. I also want to thank my committee members, Dr. Milind Deo and Dr. John McLennan, for their insights and guidance throughout the course of my graduate school career. My heartfelt gratitude to Kali Blevins for her enormous help in managing much complex data for the research. I am very grateful for her patience and willingness to meet my research goals/needs. To my colleagues, Abdul Ghani, Dhrupad Beti, William Ashley, and Nikolajs Batarags, thank you for all of your support, directly and indirectly.

Finally, much deserving gratitude to my family for all of their immense support throughout my academic journey. To my parents, Mr. and Mrs. Boakye-Yiadom, words are not enough to express my appreciation to you. To my American parents, Jeff and Patty Shields, thank you so much for providing me with an environment that helped me stay focused on my education in a foreign country. To Derek Shields, thank you very much for giving me the opportunity to realize the American dream – this one is for you. To Carlos Martines, Emmanuel Boakye Sarpong, Victor Boakye Yiadom, David Bauman, Brett Shields, Danny Wall, Colton Shields, Marcus Shields, and Bishop Phil Millet, thank you all so much from the bottom of my heart.

CHAPTER 1

INTRODUCTION

The Utica-Point Pleasant (UPP) play of Ohio lies around 1500 ft beneath the prolific Marcellus Shale. Like the Marcellus, the UPP is a gas-prone play with tremendous production potential. Across the state of Ohio, the UPP trends from the northwest towards the southeast. Production within the play dates back to the early 1800s, but recorded historical data begin from 1984. Conventional drilling and development continued until 2010, when the first unconventional horizontal drilling was completed by Chesapeake Energy. The pioneer of horizontal drilling within the play, Chesapeake Energy is the major producer within the play.

1.1. UPP Conventional Production

The Utica shale formation found in eastern Ohio consists of dark brown to black, calcareous, organic-rich shale that was deposited during the Ordovician period (Wickstrom et al., 2014). The Point Pleasant formation underlies the Utica Shale and consists primarily of interbedded limestone and calcareous shale (Wickstrom et al., 2014). Together, the Utica and Point Pleasant (UPP) formations in eastern Ohio have been touted as a significant shale play in the United States.

Although commonly referred to as the Utica Shale, major production within the

formation results from the Point Pleasant interval. Compared to the Utica Shale, the Point Pleasant has a lower clay content, higher organic content, and better porosity, thereby making it the better target (Murphy et al., 2013). Stratigraphically, the Point Pleasant lies directly above the Trenton Limestone and is thought to be equivalent to the thick deposits of the Trenton carbonate platform of northwestern Ohio, famous for the Lima-Indiana oil and gas trend, which was the first true giant field produced in North America starting in 1884 (Wickstrom et al., 2014). Throughout much of Ohio, as the Trenton Limestone thins, the UPP thickens. Thickness of the UPP is estimated to range from 150 – 200 feet (Wickstrom et al., 2012).

Total oil production in 1984 from vertical wells was estimated at just over 12MMbbl. Corresponding data show most wells either produced cumulative oil around 100bbl or failed to record oil production throughout the entire year. The majority of the wells drilled during that time were located in the Washington, Gallia, Perry, Muskingum, and Wayne Counties.

1.2. UPP Unconventional Developments and Production

According to the Ohio Department of Natural Resources (ODNR), 2318 horizontal well permits had been approved as of 12/3/2016 (Ohio Department of Natural Resources, 2017). Of these, 1473 were producing wells, 458 were permitted, 300 had been drilled, and the remaining had either been shut in/inactive or plugged and abandoned. Oil and gas production within the formation is achieved mostly by drilling long, horizontal laterals with multistage hydraulic fracturing. The first horizontal well was drilled into the UPP in Ohio in 2010 by Chesapeake Energy (Wickstrom &

Shumway, 2014). Chesapeake Energy is by far the biggest player in the trend, with Gulfport Energy a distant second, followed by Antero Resources and Ascent Resources, in that order. Chesapeake owns 825 of the total permits issued through 2016 (36%), Gulfport has 311 (13%), Antero has 210 (9%) and Ascent has 196 (8%), rounding up the top four major players within the formation (ODNR, 2017).

Historical data available from the ODNR Division of Oil & Gas Resources show that horizontal shale production has gradually increased since 2010. Shale production numbers increased from 46 Mbbl/year in 2011 to 3.9 MMbbl at the end of the third quarter of 2016 (ODNR Division of Oil & Gas Resources, 2017). A majority of the horizontal shale production occurred in the Belmont, Carroll, Columbiana, Harrison, Monroe, and Noble Counties.

Although oil production within the play has shown a gradual increase, the UPP is a gas-dominated play. Similar to other unconventional plays within the United States (Marcellus, Barnett, etc.), gas development takes precedence over oil production. Over several million years of geologic time, sediments were gradually deposited. This led to increasing burial of layers at greater depths. At these greater depths, sediments were subjected to higher temperatures (geothermal gradient) and pressures. Different environments existed, including marine, lacustrine, deltaic, and fluvial, where anoxic (depletion of dissolved oxygen) conditions prevailed. Organic matter in these sediments was subsequently converted into long chain and cyclic geological polymer-like compounds known as kerogen. The elements, carbon, hydrogen, oxygen, nitrogen, and sulfur, are considered the main constituents of kerogen, a precursor of hydrocarbons (Maende & Weldon, 2016).

Increasing burial of the kerogen environments depleted of oxygen subjected them to increasing temperatures. The burial subsequently caused the breakdown of kerogen and generation of organic carbon residue. In order to fully define the type of kerogen and its respective environment, pyrolysis is employed. Pyrolysis is a key technique in identifying and quantifying pertinent geochemical properties of a rock. It is defined as the high temperature breakdown of organic matter in the absence of oxygen (anoxic environment).

Pyrolysis of all research samples was conducted using HAWK^{TM} Resource Workstation, a product of Wildcat Technologies. A flagship instrument for Wildcat Technologies, HAWK^{TM} measures S1, S2, S3, S4, Tmax, TOC, CC, and Absolute Tmax for kinetics calculations (Wildcat Technologies, 2016). For the purpose of this research, the following key parameters were considered; S1, S2, S3, Tmax, and TOC. S1, the free oil, is the oil that is present in a rock formation, and are usually detected during the start of the pyrolysis process, typically from 50°C.

S1 is measured in mg of hydrocarbons per gram of rock (mgHC/g of rock) and a rock with a result greater than 1 is considered to be a good source rock (Wickstrom et al., 2012).

S2 measures the amount of hydrocarbons generated through thermal cracking of kerogen and heavy hydrocarbons. S2 also represents the potential of a rock to generate hydrocarbons if it were subjected to increasing burial temperatures. Measured in mgHC/g of rock, an S2 of greater than 5 is considered to represent good source rock generative potential (Wickstrom et al., 2012). S3 is the measurement of CO_2 that is generated during the pyrolysis cycle, typically between 300°C and 400°C. S3 is measured in mgCO_2/g of

rock (Wildcat Technologies, 2016).

Tmax, in °C, represents the temperature at which maximum generation of S2 hydrocarbons is achieved. It is diagnostic of the kerogen type and is a maturity measure of the rock (Wildcat Technologies, 2016).

Total Organic Carbon, TOC, measures the organic carbon richness of the rock. It is expressed in weight %. A TOC of 0.5% is generally regarded as the minimum for defining a petroleum source rock. At values greater than 1.0%, the source rock is considered to have good generating petroleum potential (Wickstrom et al., 2012).

1.3. Petroleum Quality in Oil and Gas Wells

The ability to determine the quality of oil prior to production drilling drives most investment decisions within the oil and gas industry. Definitively delineating production sweet spots ahead of production further enables all layers of an organization to make informed decisions on project investments and to carry out return on investment calculations. Many techniques have been developed to assess the organic richness, production type, and level of thermal maturity of potential source rocks. These techniques usually measure optical or chemical characteristics of the extractable and non-extractable (or kerogen) sedimentary organic matter (Dembicki Jr. et al., 1983).

The research will identify the quality (light, medium, and heavy) of oil from the above wells using a new analytical method, Incremental S1, and validate the results using gas chromatography extract techniques as a complement. The aforementioned new analytical method is detailed in the next chapter.

CHAPTER 2

PURPOSE OF THIS STUDY

In trying to understand the petroleum quality within the Utica-Point Pleasant play, a few techniques are employed in this research. The first is using the produced oil from the play to conduct gas chromatography (GC) analysis. That analysis provides hydrocarbon peaks that correspond to oil quality. The next available option in determining oil quality is using the American Petroleum Institute (API) gravity. API gravity of oil gives an idea of how heavy or light the oil is, corresponding to oil quality. The final option is using extract GC. In extract GC, oil is extracted from reservoir rocks at predetermined temperature and pressure conditions, and analyzed using GC. A two-step process, extract GC is very useful in predicting oil quality within any play.

However, using a conventional pyrolysis method to understand area of fluid windows and oil presence, and employing a newly developed analytical method to screen the windows for oil quality, a less time-consuming and cost-effective option is possible for understanding and predicting oil quality.

2.1. Understanding Oil Quality in the Utica Play

Understanding the quality of oil within the UPP play enables the resolution of limited oil drilling activities within the play. Unfortunately, the play is gas-prone and

hence the unavailability of produced fluids for GC analysis, to help understand oil quality within the play. Although some of the wells fall within the oil window, there is very limited oil production for determining the API gravity of the oil or the gas-oil ratio (GOR), which will lead to understanding oil quality.

In order to remain economically efficient, while generating accurate oil quality predictive data for the UPP play, pyrolysis was used to understand the area of fluid window and oil present. Once the oil presence and fluid window have been established, a newly developed analytical method, Incremental S1 (IS1), was used to screen the fluid windows for oil quality. Data generated using IS1 were compared to extract GC results. With this set of data combinations, a better understanding of oil quality within the UPP was established.

CHAPTER 3

METHODS

The first step in selecting wells for core sampling involved analyzing available geochemical data for existing wells within the play. Once geochemical data collection was completed, the next step involved analyzing and identifying all wells within the different fluid type windows; low maturity, oil maturity, and condensate maturity. The final step was finding out core availability for all wells within the different fluid type windows. Combining the aforementioned steps resulted in selecting four wells for this research. Continuous feet of core were sampled from the four selected wells. HAWK pyrolysis was conducted on all samples, after which subsamples were analyzed using IS1, the newly developed method that analyzes samples faster and gives visual representations of S1 signal peaks. Figure 3.1 is an image of the HAWK instrument.

3.1. Core Sampling

A visit to the ODNR repository was made to sample cores from the four selected wells. A well each from Wyandot (API # 34-175-202870000), Marion (API # 34-101-201960000), Tuscarawas (API # 34-157-253340000), and Washington (API # 34-167-297200100) Counties make up the four wells sampled for the research. Figure 3.2 is an ONDR-generated map showing locations of these wells, as well as their locations within

the various fluid windows. Originally based on vitrinite reflectance for maturity delineation, Tmax data from pyrolysis analysis were used to assist in validating the designated fluid maturity windows. From Figure 3.2, Wyandot and Marion Counties fall within the low maturity window. Tmax results for analyzed samples from Wyandot County ranged from a low of 428°C to a high of 435°C. Marion County samples have Tmax values from 427°C to 433°C. Tuscarawas County, which falls within the oil maturity window as shown in Figure 3.2, has Tmax values from 446°C to 453°C. Washington County samples, located within the condensate maturity fluid window, generated Tmax values from 313°C to 623°C. Using available well logs as reference, wells were sampled to cover depths from the Utica Shale through to the Trenton or Lexington Limestones. In addition to establishing the depths of coverage, wells were sampled at 2ft intervals at 20g per sample.

3.2. Core Sample Preparation

At the aforementioned sampling depths, a total of 190 samples were requested from the ODNR core lab. The division of samples between the four wells is as follows; 40 core samples were taken from Wyandot (API # 34-175-202870000), 60 core samples were taken from Marion (API # 34-101-201960000), 3 sidewall cores were taken from Tuscarawas (API # 34-157-253340000), and 87 core samples were taken from Washington (API # 34-167-297200100). The samples were split, storing a parent sample and preparing the subsample for pyrolysis.

In order to prepare the samples for pyrolysis, each of the core samples are first ground to 60 mesh size using a porcelain mortar and pestle, and a 60 mesh sieve to

confirm ground size. To avoid sample contamination during grinding, the mortar and pestle are thoroughly cleaned between grinding samples. Once ground and the samples meet the size, they are weighed on a 4-decimal-place-capable balance. Recommended weight per sample is about 70 mg. However, smaller weights are typically used for very organic rich samples in order to avoid saturating the HAWK's detectors.

3.3. HAWK™ Pyrolysis

Pyrolysis and oxidation for determining and understanding key geochemical parameters of source rock were first introduced by Espitalié et al. in 1977 (Espitalie, Deroo, & Marquis, 1985). Subsequently, the working performances and developments of Rock-Eval® were discussed in studies such as Espitalié et al. in 1985, 1986a, 1986b; Bordenave in 1993; and Larfargue et al. in 1998. Rock-Eval equipment has undergone many technical improvements over the subsequent decades, with the latest version being Wildcat Technology's flagship instrument, HAWK™.

Currently, the most common and widely used temperature program in pyrolysis is PyrosS3650_TOC750. This conventional method is used for the evaluation of S1-free oil, S2-kerogen yield, S3, Tmax, and TOC. PyroS3650_TOC750 has two parts to it, the pyrolysis and oxidation modes. The temperature curve for PyroS3650_TOC750 is shown in Figure 3.3. In pyrolysis, the initial oven temperature is at 100°C, with an initial purge time of 5 minutes. The sample for analysis is then introduced into the oven and subjected to 3 minutes of initial pyrolysis isotherm of 300°C. From there, a pyrolysis rate of 25°C/min is maintained until the final pyrolysis temperature of 650°C is attained. In this mode, an inert gas (Helium) is used as a carrier gas at a flow rate of 100ml/min. The gas

passes through the pedestal, then sweeps through the sample crucible in the oven. The Helium gas is then sent to a Flame Ionization Detector (FID) to detect the quantity of sample ionized in the hydrogen flame.

As sample ionization is occurring, a split flow rate of 40 ml/min is continuously being sampled and sent through a filter, to a moisture trap attached to the HAWK^{TM}, and to the Infrared (IR) detectors for detection of the amounts of carbon dioxide and carbon monoxide in the samples. In oxidation, an initial temperature of 300°C is maintained for 1 minute. Then at a rate of 25°C/min, sample is heated to 750°C, and held at this temperature for 5 minutes. Together with purge times, this conventional method lasts for a total of 46 minutes per sample. In this oxidation mode, air is used as the carrier gas at a flow rate of 250ml/min, while a two-way split is used to sweep a portion of gas at a split flow rate of 50ml/min. The gas being swept is sent to IR detectors to detect the volume amounts of carbon dioxide and carbon monoxide. The split flow schematic of the Hawk system is shown in Figure 3.4. All 190 ground subsamples were analyzed using the conventional pyrolysis method.

3.4. Incremental S1 (IS1)

As this research focuses on determining oil quality within the UPP, subsamples from the HAWK pyrolysis method that yielded an S1 (free oil) value of one or greater 1 mgHC/g of rock were further analyzed using a newly developed analytical method, Incremental S1.

IS1 (Incremental S1), has been developed to quickly and effectively analyze source rock potential (Beti, 2016). Unlike the conventional pyrolysis method, IS1

analyzes a sample for 30 minutes, saving significant time and expediting data acquisition and processing. Additionally, instead of generating a single S1 peak as in the conventional method, IS1 enhances the S1 peak, and generates six different local S1 peaks (IS1_1 to IS1_6). These enhanced S1 peaks provide the possibility for understanding hydrocarbon chains lengths and/or distributions within the analyzed sample. The temperature profile of this new analytical method is shown in Figure 3.5.

A modification of the conventional (PyroS3650_TOC750) method, IS1 consists of six, 5-minute isotherms at 50°C, 100°C, 150°C, 200°C, 250°C, and 300°C, with a temperature rate of 200/min after every 50°C interval (from 50°C to 100°C, 100°C to 150°C, up until 300°C). IS1 can be used to predict the API gravity of a reservoir source rock using measurements of refractive index and boiling points of the hydrocarbon molecules. Subsamples for the 31 samples with S1>1 mgHC/g of rock were analyzed using IS1.

3.5. Extract GC and GC Analysis

From the 31 samples that were analyzed using IS1, six samples were selected for Extract GC or solvent extraction analysis. Two of these samples were from Wyandot County (EGI.Nov.2016.00316 and EGI.Nov.2016.00330 (3374)), one from Marion County (EGI.Nov.2016.00363 (3372)), one from Tuscarawas County (EGI.Nov.2016.00200 (3548)), and the final two from Washington County (EGI.Nov.2016.00209 and EGI.Nov.2016.00222 (8004)). Solvent extraction solvates the free compounds and isolates them from the kerogen and mineral matrix (Wright et al. 2015). The solvent most widely used in this extraction phase is dichloromethane (DCM).

Once the DCM application is completed, a GC technique is used to separate complex mixtures into individual compounds. The FID and mass-spectrometry quantify the compounds and identify any unknown compounds, respectively.

For this portion of the research, the six samples were sent to GeoMark Research for the extraction and GC analysis.

Figure 3.1: Wildcat Technology's HAWK, used in all pyrolysis analyses that were performed (Wildcat Technologies, 2016).

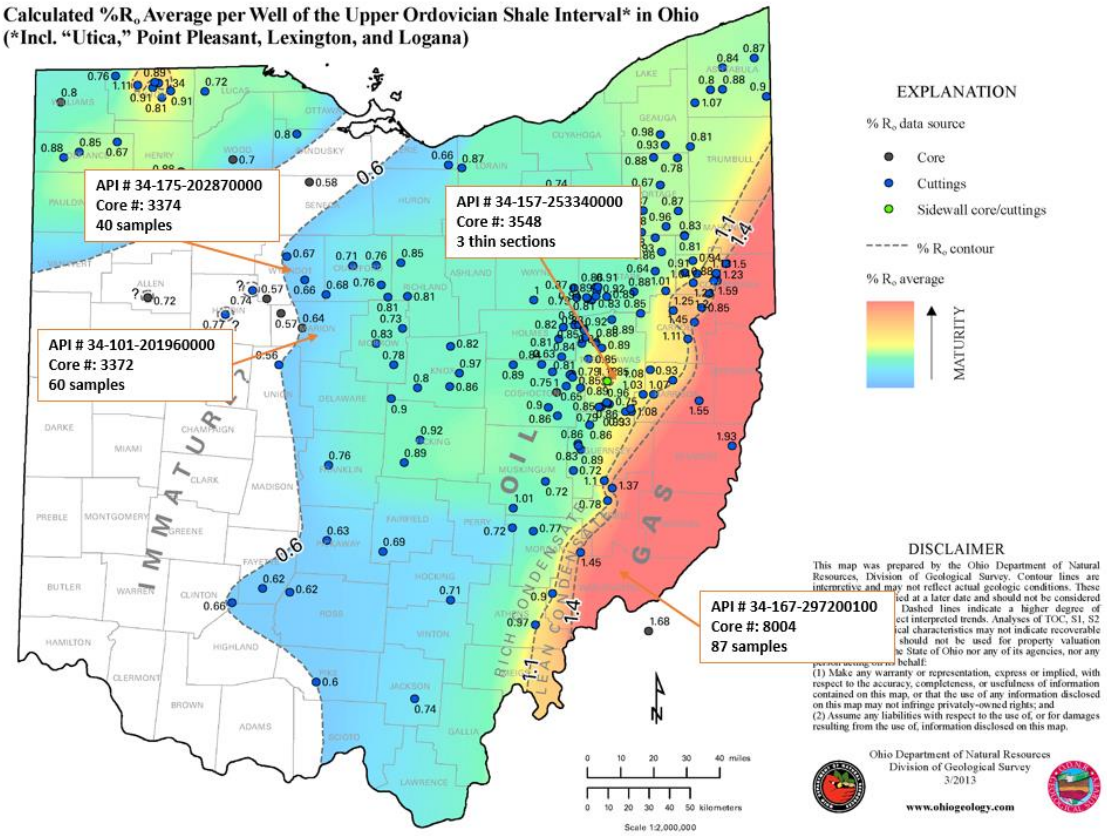

Figure 3.2: Core sampling locations overlaid on %R_o maturity map of Ohio – modified from Ohio Division of Geological Survey's Upper Ordovician Shale Maturity Map of Ohio. The map shows two wells from Wyandot and Marion Counties within the low maturity fluid window. A single well from Tuscarawas County falls within the oil maturity window, and the final well from Washington County falls within the condensate maturity window (Ohio Division of Geological Survey, 2013).

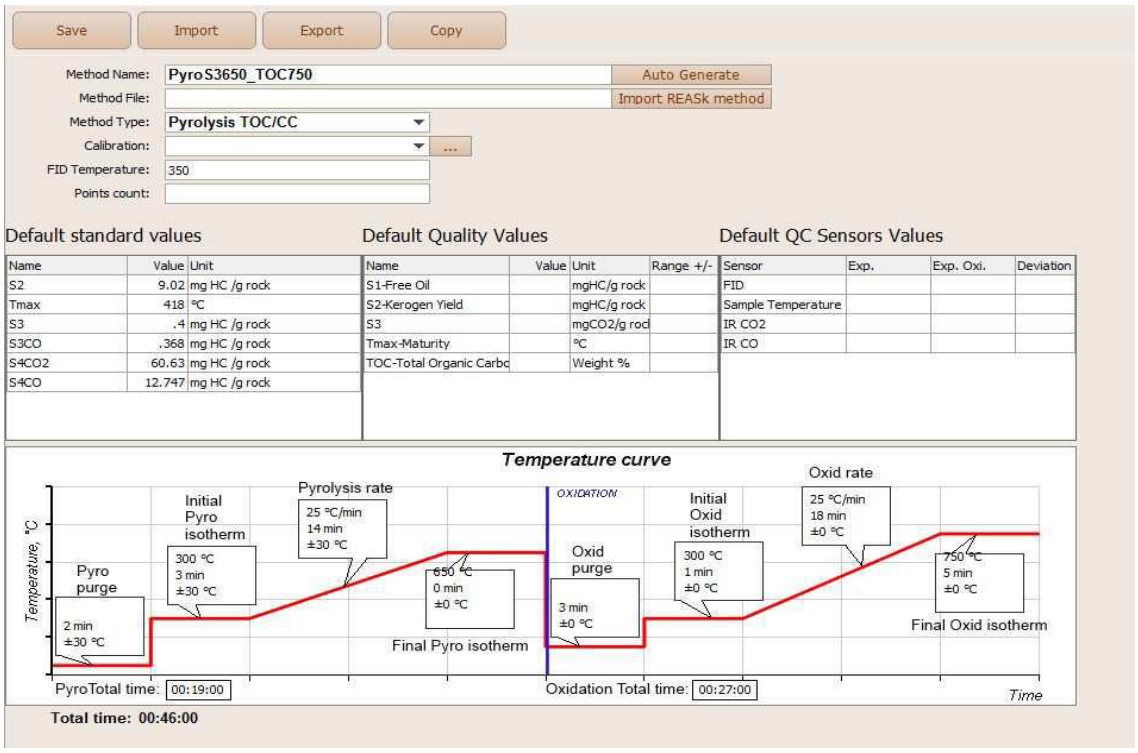

Figure 3.3: Temperature profile curve for the conventional pyrolysis method, PyroS3650_TOC750 (Wildcat Technologies, 2015).

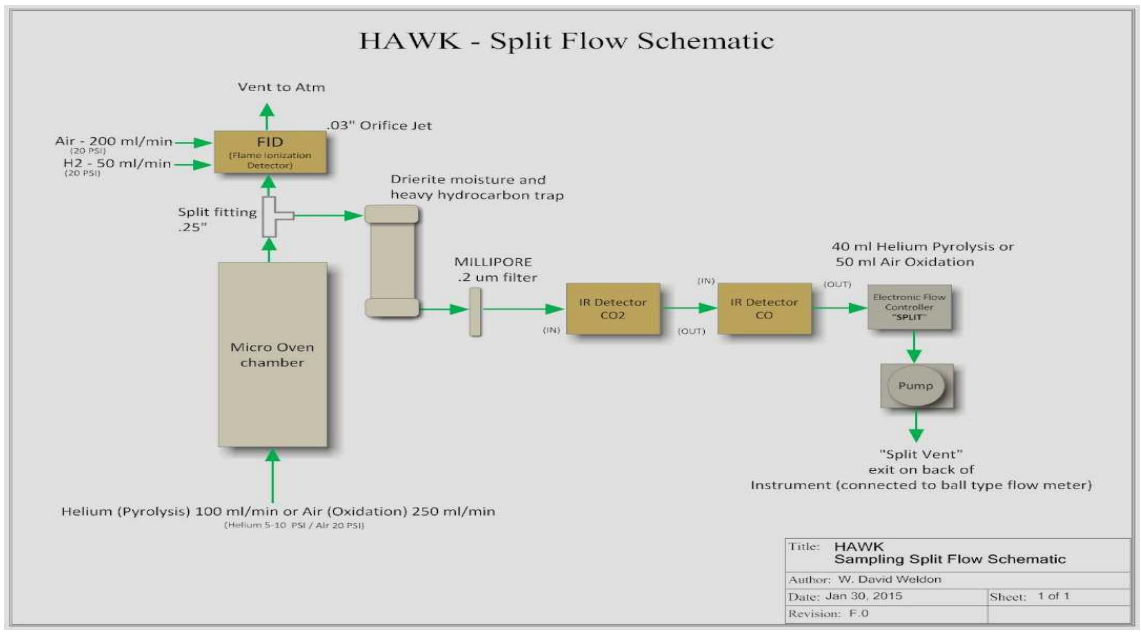

Figure 3.4: Split Flow Schematic of the HAWK Pyrolysis Machine (Wildcat Technologies, 2015).

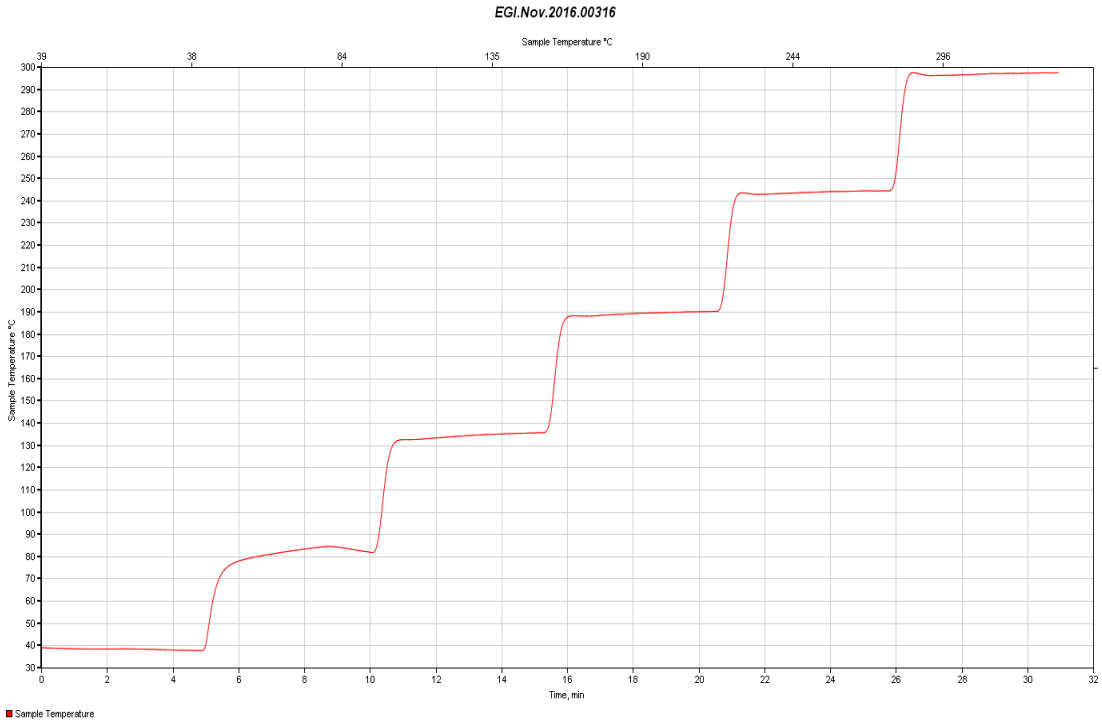

Figure 3.5: A typical sample temperature profile curve for the newly developed pyrolysis method, Incremental S1. The figure shows six 5-minute isotherms beginning at 50°C.

CHAPTER 4

RESULTS

This chapter presents key results from the research. Pertinent plots of TOC, HI (Hydrogen Index), OI (Oxygen Index), S1, and S2 will be presented. IS1 results will detail the significant shift in S1 peaks for samples in the low maturity, oil maturity, and condensate maturity windows. A ternary plot will show a variation of S1 values across the four wells. Extract GC results will also highlight the difference in maturity levels for all of the samples analyzed in this research.

4.1. Hawk Pyrolysis

Initial pyrolysis of the 190 samples using the conventional method provided pertinent geochemical parameters that helped delineate wells based on maturity. Of the samples analyzed, 100 samples were in the low maturity fluid window, three samples fell in the oil maturity fluid window, and the remaining 87 samples were in the condensate maturity fluid window. Detailed pyrolysis results for all wells are tabulated in Appendices A through D.

Figure 4.1 is a plot of depth versus TOC for all of the samples analyzed using the conventional pyrolysis method. Figure 4.2 shows kerogen quality by using a standard plot of hydrogen index (HI) versus oxygen index (OI) for all samples.

Figures 4.3 and 4.4 are track of S1 and S2 with depth, respectively, for all of the samples analyzed with the conventional pyrolysis method. Figure 4.5 is a plot of free oil (S1) versus Tmax, and Figure 4.6 shows normalized oil content for all samples analyzed using the conventional pyrolysis method.

In addition to the aforementioned plots of key geochemical parameters, a map of maximum S1 and average Tmax were generated for all four wells. Figure 4.7 and 4.8 are maps of the State of Ohio showing the locations of the wells and sorted according to their respective S1 and Tmax values.

4.2. Incremental S1 (IS1)

The purpose of the research is to predict the oil quality within the Utica-Point Pleasant formation. S1, representative of free oil, is a key parameter in this research. During reservoir prospecting, S1 value greater than 1 mgHC/grock is considered to be indicative of a good reservoir rock. IS1 helps screen the various fluid windows for oil quality (light, medium, or heavy), and relies heavily on the amount of free oil within a reservoir rock. In order for a sample to be analyzed using IS1, a criterion was set at 1 mgHC/grock. After applying the criterion to results generated from the conventional pyrolysis method, 31 samples warranted further IS1 analysis. Detailed results from IS1 analysis on these 31 samples are tabulated under Appendix E.

Raw FID signals for six of the 31 samples analyzed using IS1 are presented below. These six samples were also further analyzed using GC Extract (see Section 3.5). Figures 4.9 through 4.14 are FID signals for these samples. The figures present peak (S1_1 to S1_6) distributions from each fluid window.

In addition to signal peaks, a ternary plot of Sh, Sm, and S1, representative of the fractions of petroleum released at three different temperature ranges, is presented in Figure 4.15. Detailed IS1 experimental results from the HAWK^{TM} for the ternary plot are provided in Appendix E.

4.3. Extract GC

The purpose of this research is to use an inexpensive analytical method to help define and predict petroleum quality based on light, medium, or heavy. After screening the various fluid windows for oil maturity using IS1, a technique to complement and help refine oil quality within the Utica-Point Pleasant play, extract GC is employed. Six samples representing the various fluid maturity windows were sent to GeoMark Research for measurements. The samples included two from Well 3374 (low maturity fluid window), one from Well 3372 (low maturity fluid window), one from Well 3548 (oil maturity fluid window), and two from Well 8004 (condensate maturity fluid window). Figures 4.16 through 4.21 are extract GC results for these six samples. From these measurements, a ternary plot for all of the eluted compounds during the extraction process is shown in Figure 4.22. This figure shows the distribution of carbon compounds, relative to the low, oil, and gas fluid maturity windows. Detailed extract GC data for generating the ternary plot are provided in Appendix F.

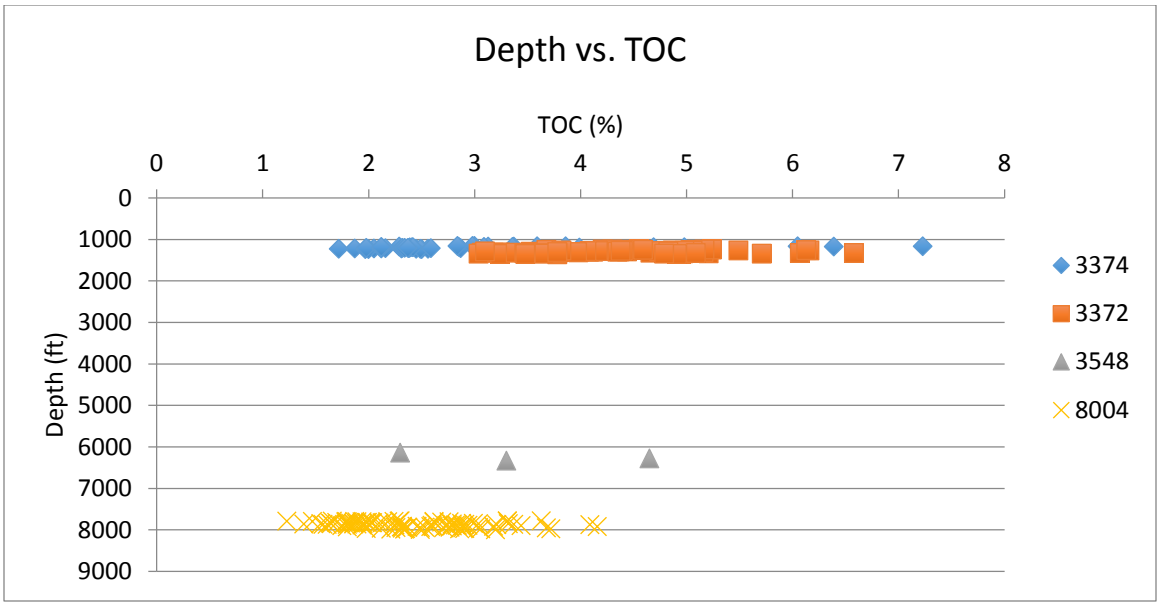

Figure 4.1: A plot of depth versus TOC for all samples analyzed using the conventional pyrolysis method, PyroS3650_TOC750. Well 3374 and 3372 fall within the low maturity window (Figure 3.2 and Section 3.1). Wells 3548 and 8004 fall within the oil and condensate maturity fluid windows, respectively.

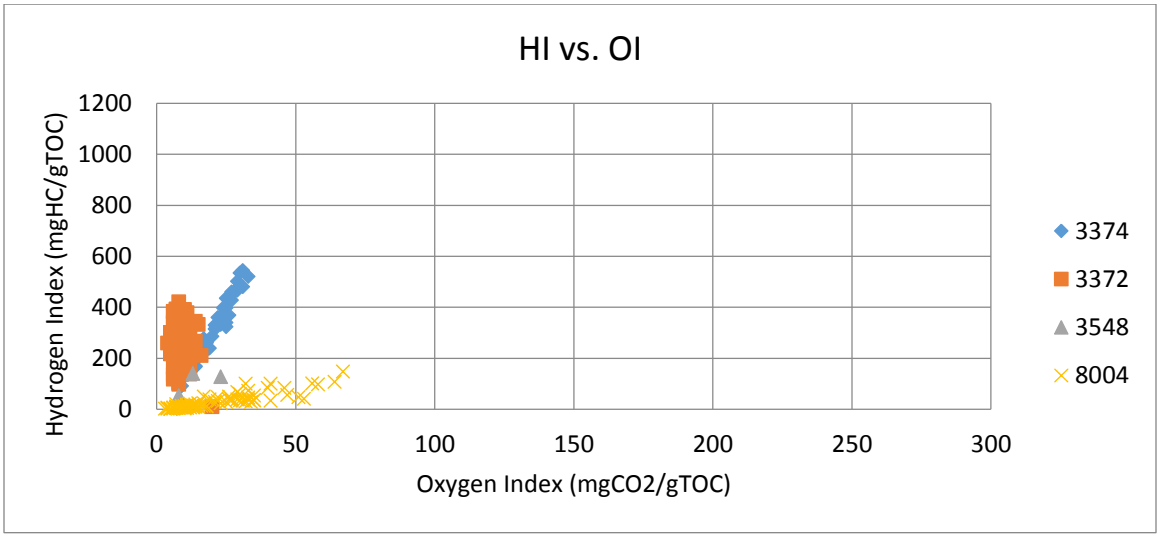

Figure 4.2: A plot of HI versus OI for all samples analyzed using the conventional pyrolysis method. The plot is also a representation of kerogen quality. Well 3374 and 3372 fall within the low maturity window (Figure 3.2 and Section 3.1). Wells 3548 and 8004 fall within the oil and condensate maturity fluid windows, respectively.

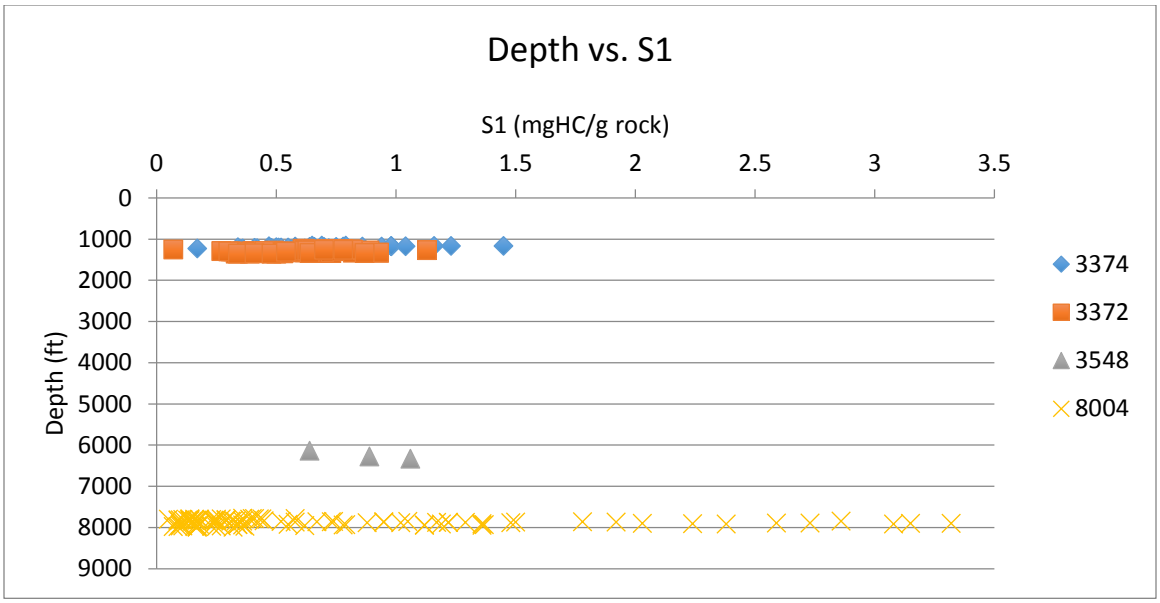

Figure 4.3: A plot of depth versus S1 for all samples analyzed using the conventional pyrolysis method. Well 3374 and 3372 fall within the low maturity window (Figure 3.2 and Section 3.1). Wells 3548 and 8004 fall within the oil and condensate maturity fluid windows, respectively.

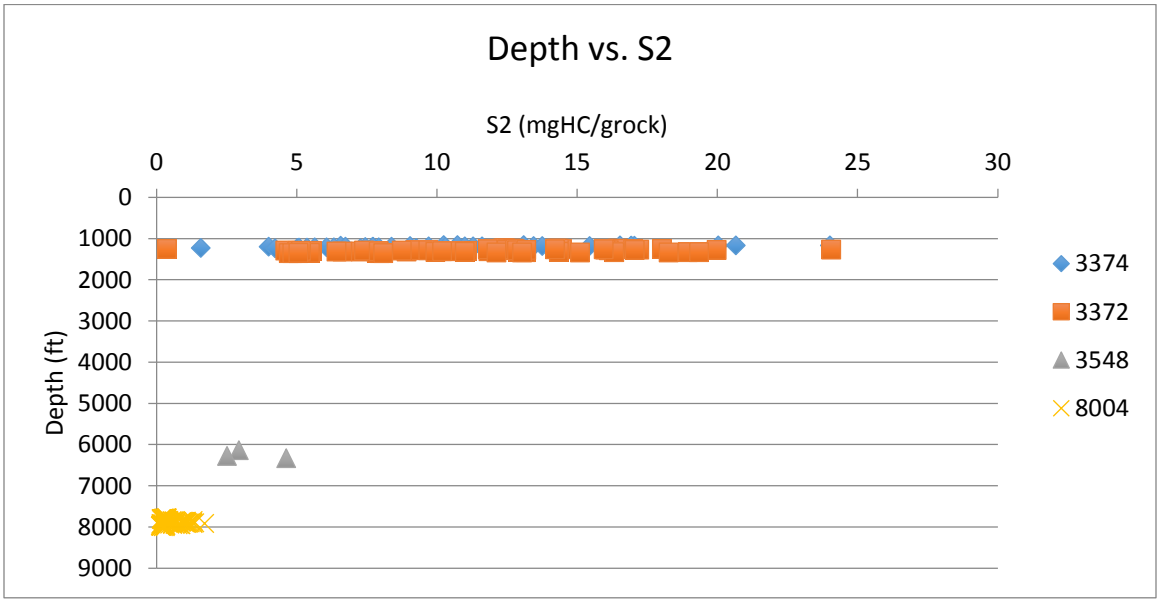

Figure 4.4: A plot of depth versus S2 for all samples analyzed using the conventional pyrolysis method. Well 3374 and 3372 fall within the low maturity window (Figure 3.2 and Section 3.1). Wells 3548 and 8004 fall within the oil and condensate maturity fluid windows, respectively.

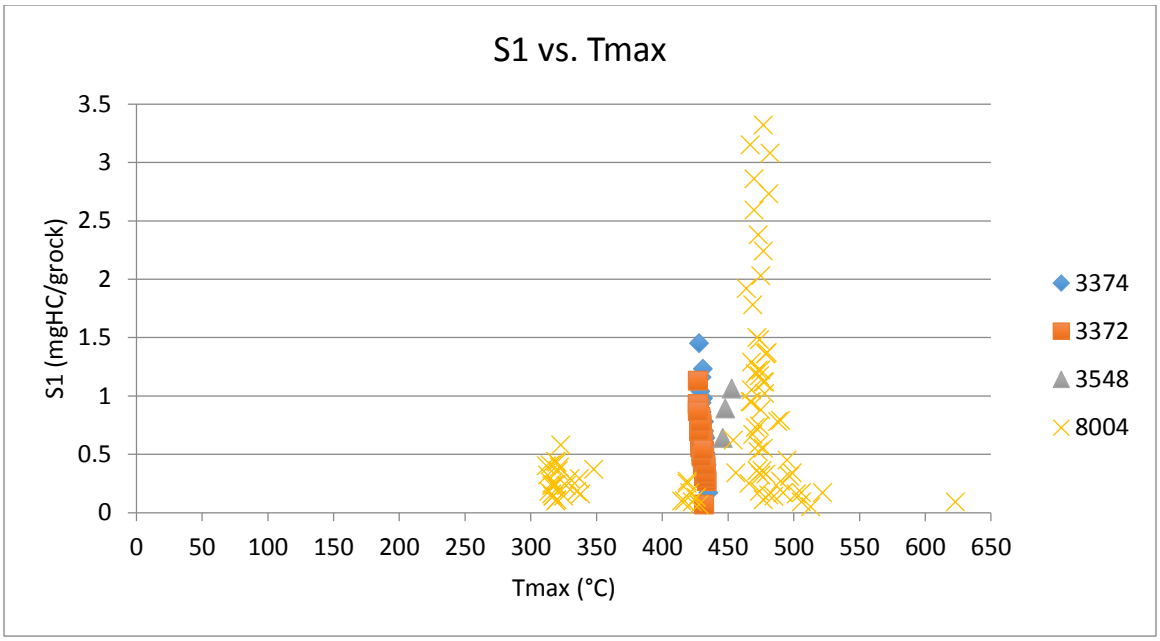

Figure 4.5: A plot of S1 versus Tmax for all samples analyzed using the conventional pyrolysis method. Well 3374 and 3372 fall within the low maturity window (Figure 3.2 and Section 3.1). Wells 3548 and 8004 fall within the oil and condensate maturity fluid windows, respectively.

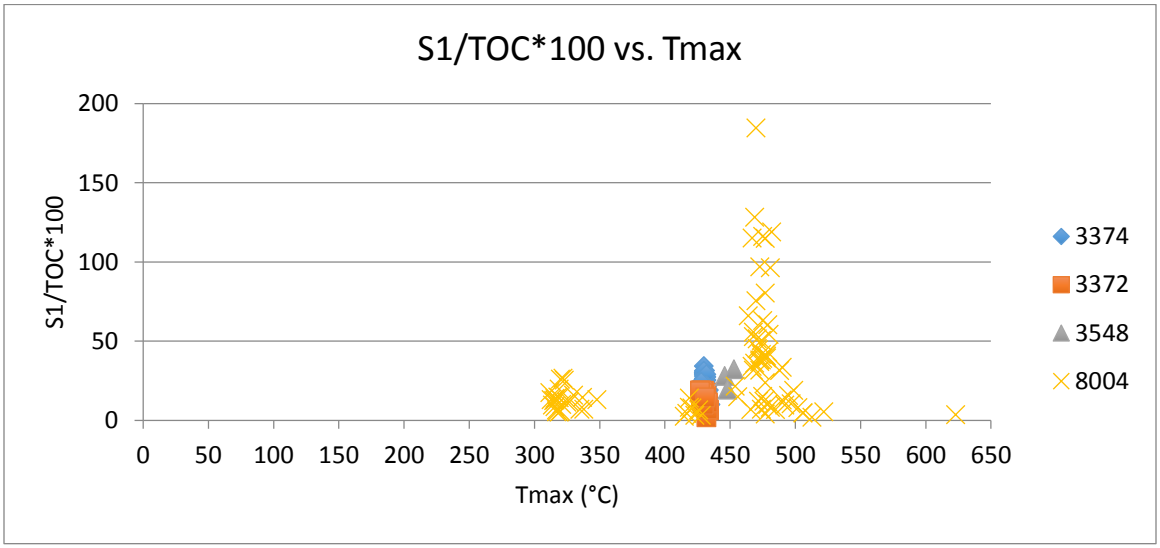

Figure 4.6: A plot of S1/TOC*100 versus Tmax for all samples analyzed using the conventional pyrolysis method. This plot also is a representation of normalized oil content. Well 3374 and 3372 fall within the low maturity window (Figure 3.2 and Section 3.1). Wells 3548 and 8004 fall within the oil and condensate maturity fluid windows, respectively.

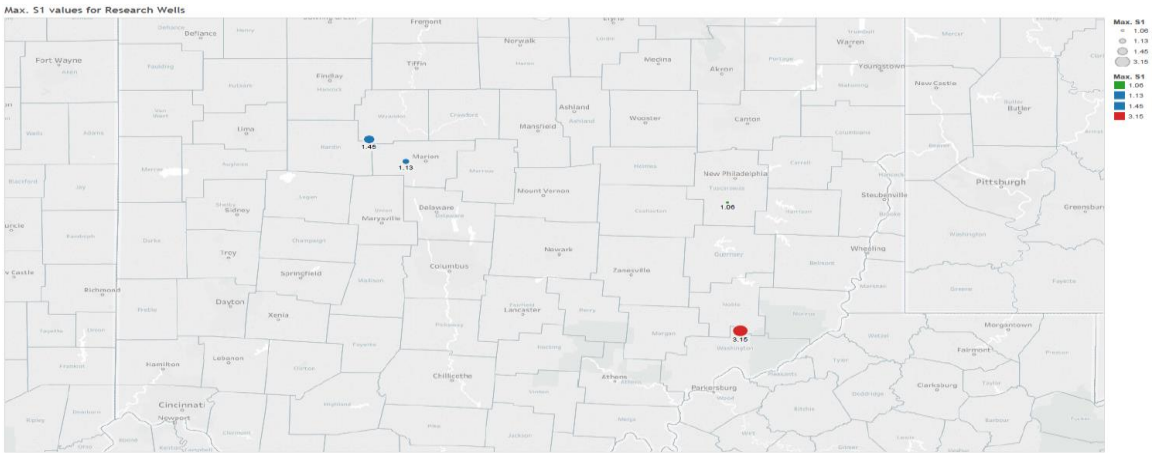

Figure 4.7: A map of the State of Ohio showing well locations. The map also depicts the maximum S1 value for each well. The red dot represents the maximum S1 value from Well 8004, found within the condensate maturity fluid window. The northernmost blue dot represents the maximum S1 value from Well 3374, found within the low maturity fluid window. The green dot represents the maximum S1 value from Well 3548, found within the oil maturity fluid window. The smaller blue dot represents the maximum S1 value from Well 3372, found within the low maturity fluid window.

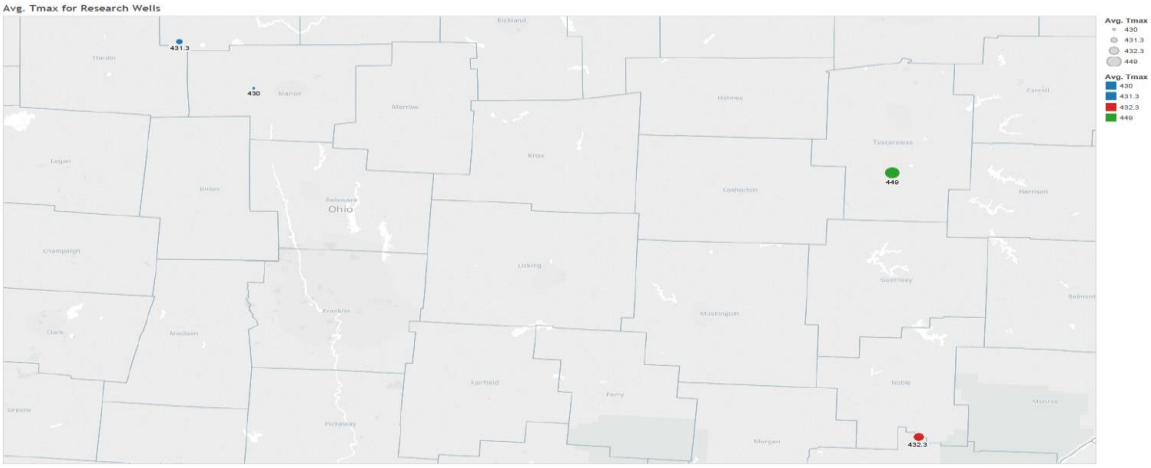

Figure 4.8: A map of the State of Ohio showing well locations. The map also depicts the average Tmax value for each well. The red dot represents the average Tmax value from Well 8004, found within the condensate maturity fluid window. The northernmost blue dot represents the average Tmax value from Well 3374, found within the low maturity fluid window. The green dot represents the average Tmax value from Well 3548, found within the oil maturity fluid window. The smaller blue dot represents the maximum S1 value from Well 3372, found within the low maturity fluid window. It must be noted that due to limited core availability for Well 3548, only three samples were analyzed, and hence the average is only representative of three samples, while the rest of the wells average over 40 samples each.

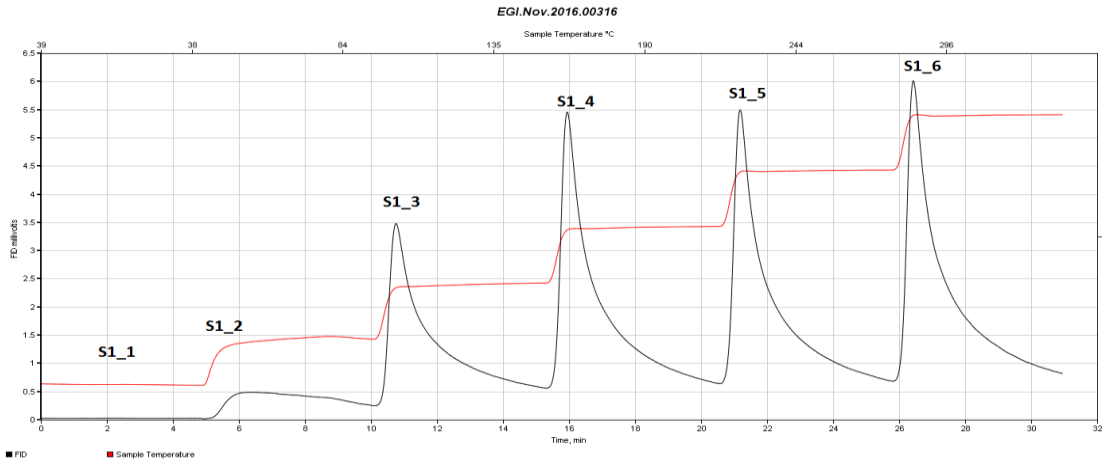

Figure 4.9: Raw FID signal for one of two samples from Core #3374 (API: 34-175-202870000) using the IS1 method, showing the six zones representative of the 5-minute isotherms beginning at 50°C. The sample falls within the low maturity fluid window (see Figure 3.2). Also in this figure, S1_6 has the predominant signal, followed by S1_5 and S1_4. FID scale has a maximum value of 6.5. Initial oil quality interpretation is heavy.

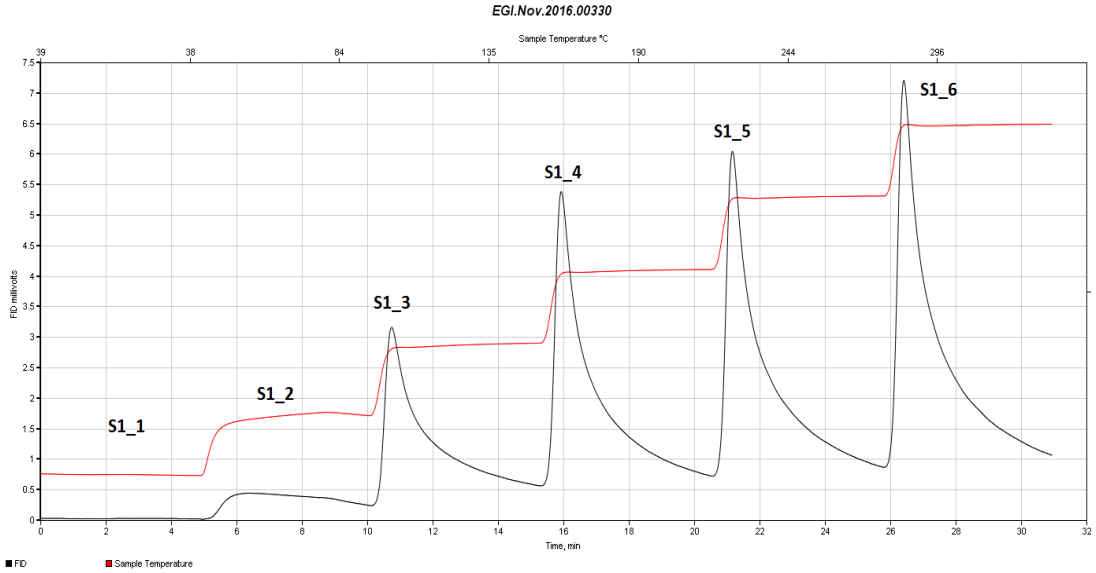

Figure 4.10: Raw FID signal for two of two samples from Core #3374 (API: 34-175-202870000) using the IS1 method, showing the six zones representative of the 5-minute isotherms beginning at 50°C. The sample falls within the low maturity fluid window (see Figure 3.2). Also in this figure, S1_6 has the predominant signal, followed by S1_5 and S1_4. FID scale has a maximum value of 7.5. Comparatively, the peak distribution patterns with Figure 4.9 are the same. However, the FID scale is higher in Figure 4.10 than in 4.9 (7.5 to 6.5). Initial oil quality interpretation is heavy.

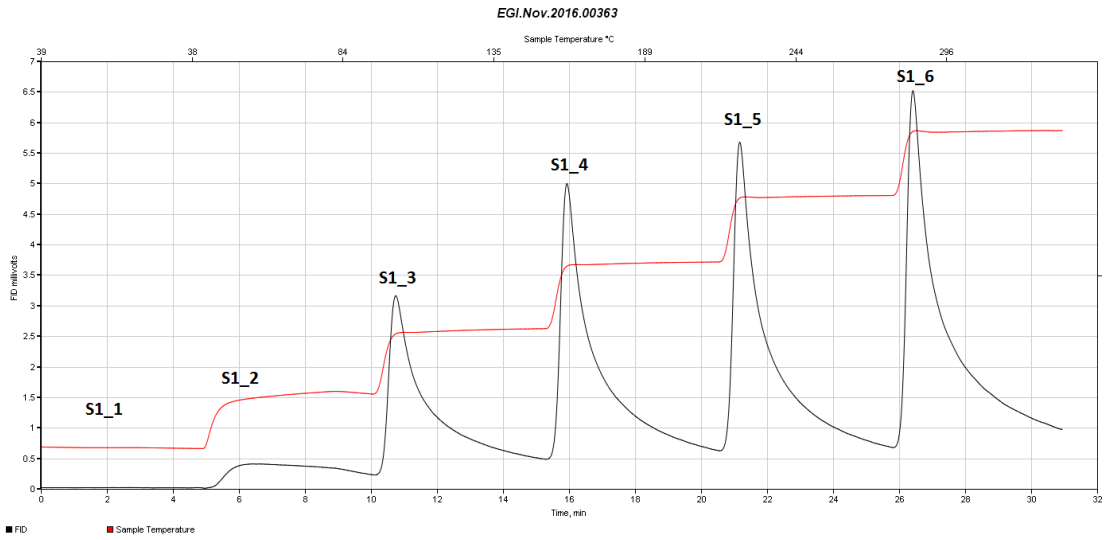

Figure 4.11: Raw FID signal for a sample from Core #3372 (API: 34-101-201960000) using the IS1 method, showing the six zones representative of the 5-minute isotherms beginning at 50°C. The sample falls within the low maturity fluid window (see Figure 3.2). Also in this figure, S1_6 has the predominant signal, followed by S1_5 and S1_4. FID scale has a maximum value of 7.0, with S1_6 value of 6.5. Initial oil quality interpretation is heavy.

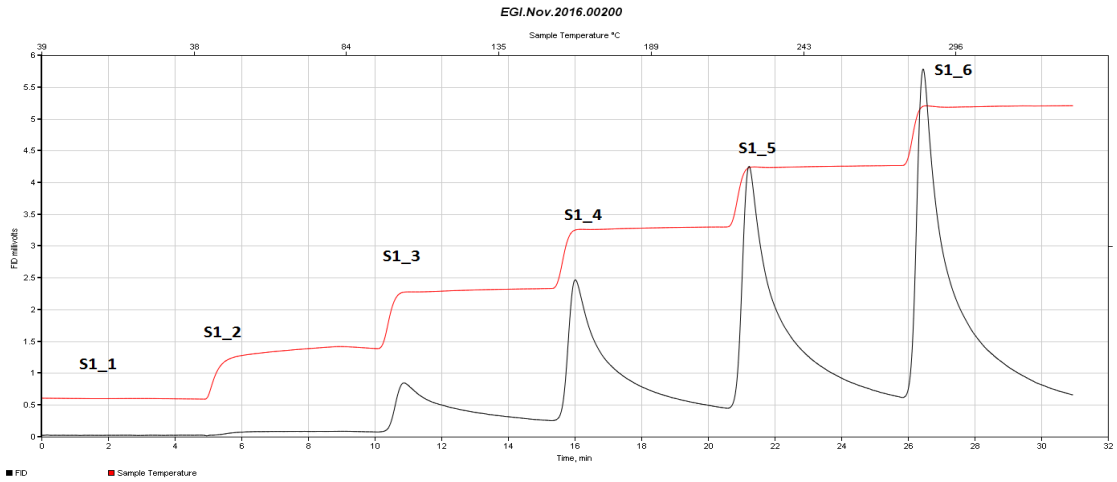

Figure 4.12: Raw FID signal for a sample from Core #3548 (API: 34-157-253340000) using the IS1 method, showing the six zones representative of the 5-minute isotherms beginning at 50°C. The sample falls within the oil maturity fluid window (see Figure 3.2). Also in this figure, S1_6 has a distinctively higher signal peak, compared to the other trailing peaks. This figure is similar to the other two figures in the low maturity fluid window, in terms of peak patterns, but the difference between individual peaks varies significantly in this figure from the other three within the low maturity fluid window. Initial oil quality interpretation is heavy.

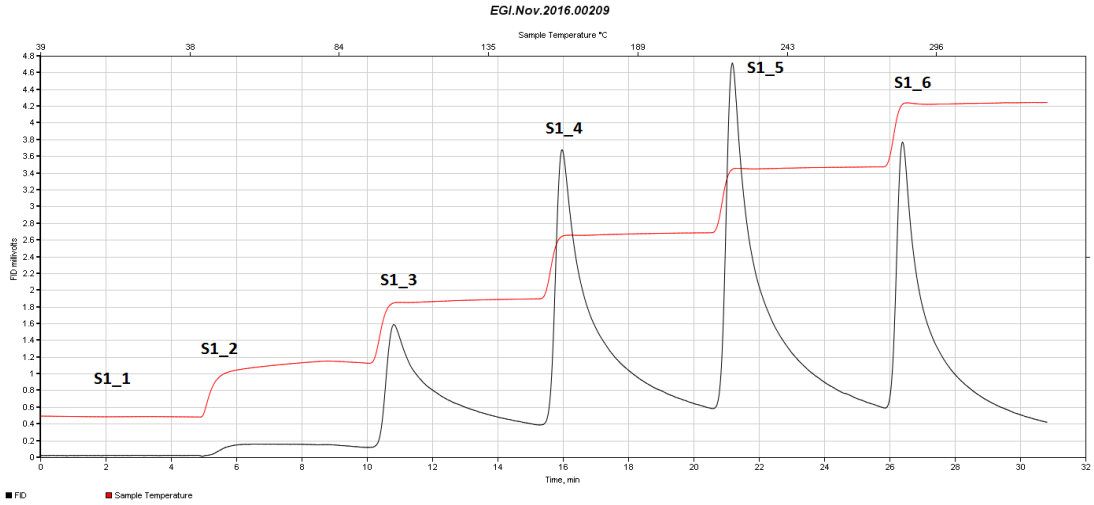

Figure 4.13: Raw FID signal for one of two samples from Core #8004 (API: 34-167-297200100) using the IS1 method, showing the six zones representative of the 5-minute isotherms beginning at 50°C. The sample falls within the condensate maturity fluid window. Also in this figure, S1_5 is the dominant signal, followed by S1_6 and S1_4. As expected for gas samples, peak distribution varies significantly compared to samples from the low and oil maturity windows. Initial oil quality interpretation is medium.

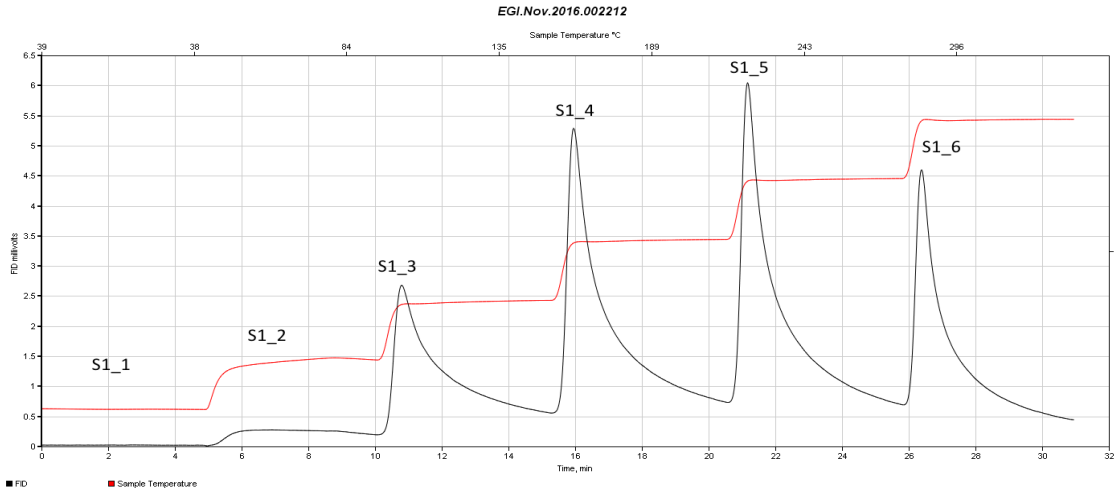

Figure 4.14: Raw FID signal for one of two samples from Core #8004 (API: 34-167-297200100) using the IS1 method, showing the six zones representative of the 5-minute isotherms beginning at 50°C. The sample falls within the condensate maturity fluid window. Also in this figure, S1_5 is the dominant signal, followed by S1_4 and S1_6. As expected for gas samples, peak distribution varies significantly compared to samples from the low and oil maturity windows. Maximum FID scale is higher in this figure than the previous figure within the condensate maturity window (6.5 to 4.8). The distinction is very clear that condensate maturity fluid window samples do not follow consistent patterns (compared to Figure 4.13). Initial oil quality interpretation is medium.

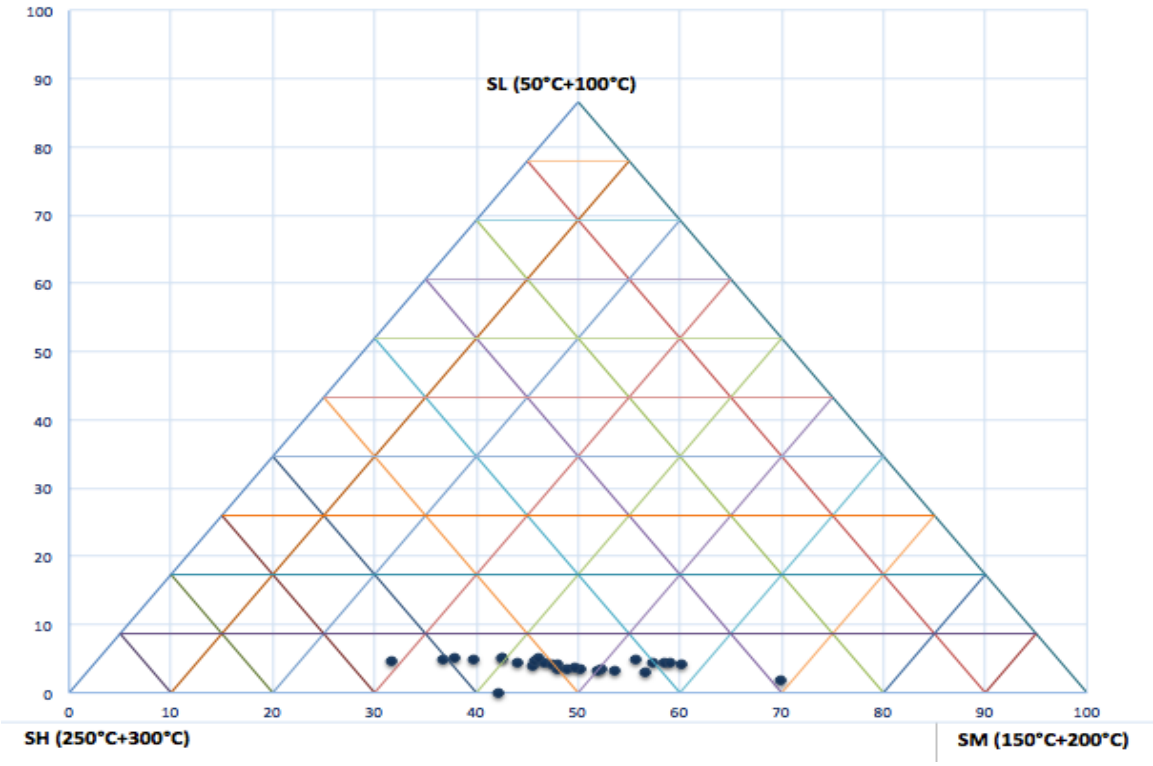

Figure 4.15: Ternary plot of Sh, Sm, and S1, showing the fractions of petroleum released at three different temperature ranges for all 31 samples analyzed using the IS1 pyrolysis method. As can be seen from the plot, most of the samples are categorized according to the following: Sl = 5%, Sm = 50%, and Sh = 45%. Initial oil quality interpretation is that the wells will produce medium to heavy oil.

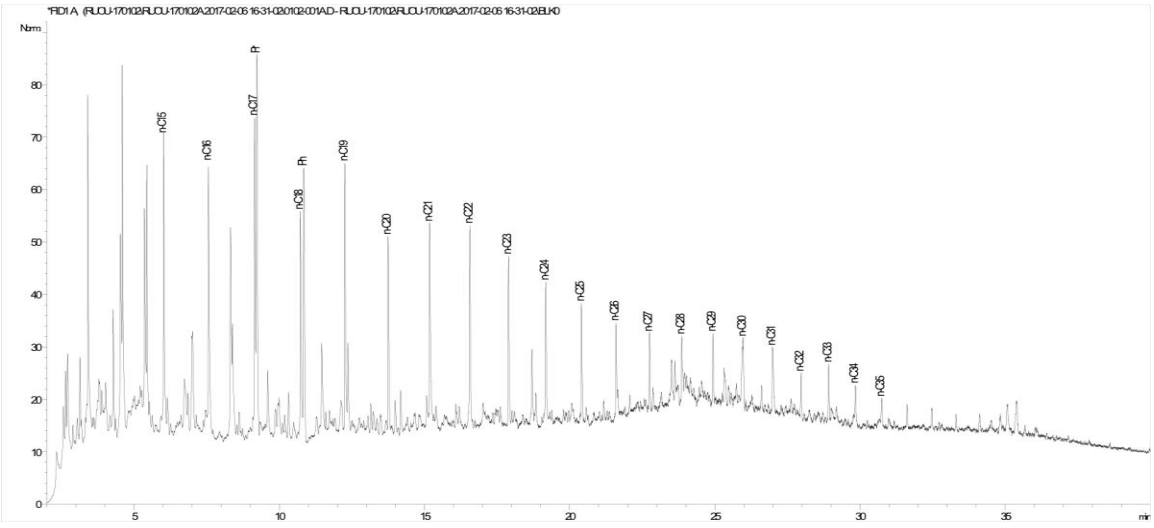

Figure 4.16: Extract GC results of one of two samples from Well 3374 in Wyandot County and located within the low maturity fluid window. The chromatogram shows C15 through C35 compounds, with the GC fingerprint showing paraffin cracking at the 24-minute mark (see Section 5.3 for explanation for the loss of less than C15 compounds).

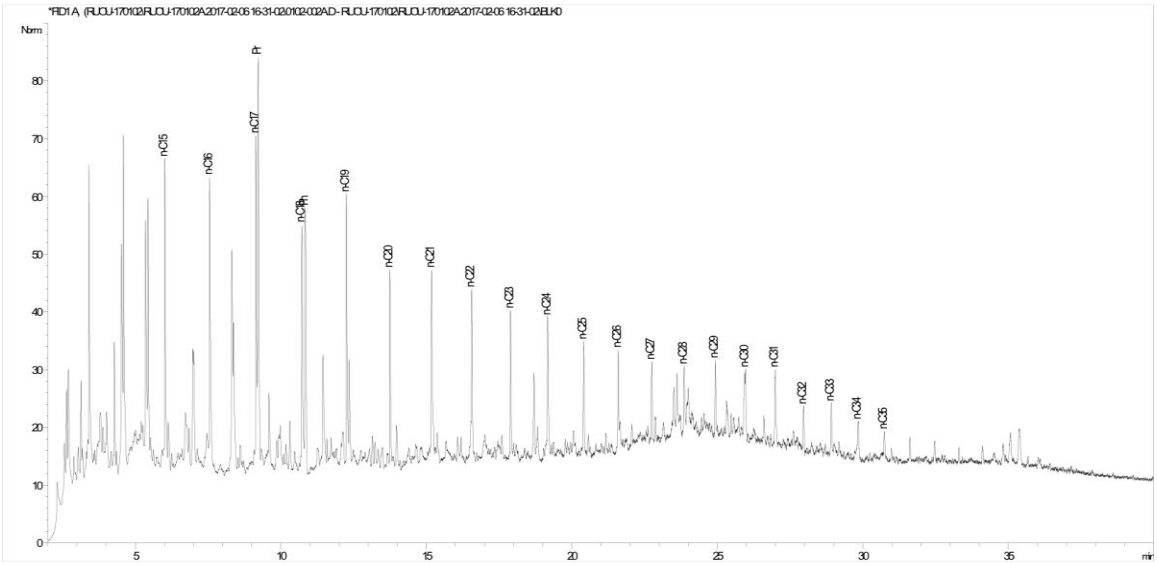

Figure 4.17: Extract GC results of the final sample from Well 3374 in Wyandot County and located within the low maturity fluid window. The chromatogram shows C15 through C35 compounds, with the apparent display of paraffin cracking at the 24-minute mark (see Section 5.3 for explanation for the loss of less than C15 compounds).

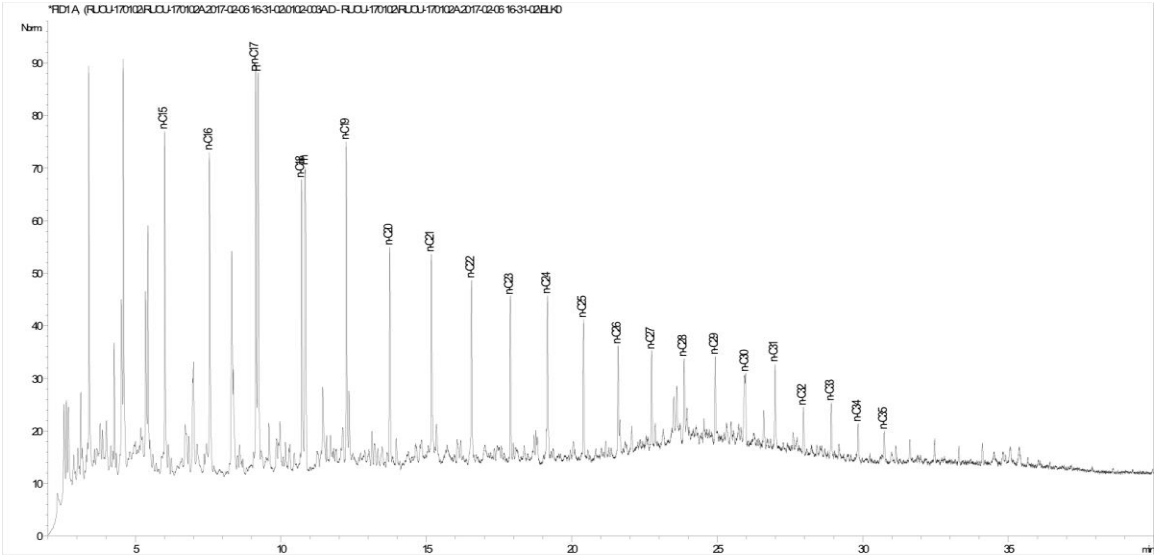

Figure 4.18: Extract GC results of the one sample from Well 3372 in Marion County and located within the low maturity fluid window. The chromatogram shows C15 through C35 compounds, with paraffin cracking observed at the 24-minute mark (see Section 5.3 for explanation for the loss of less than C15 compounds).

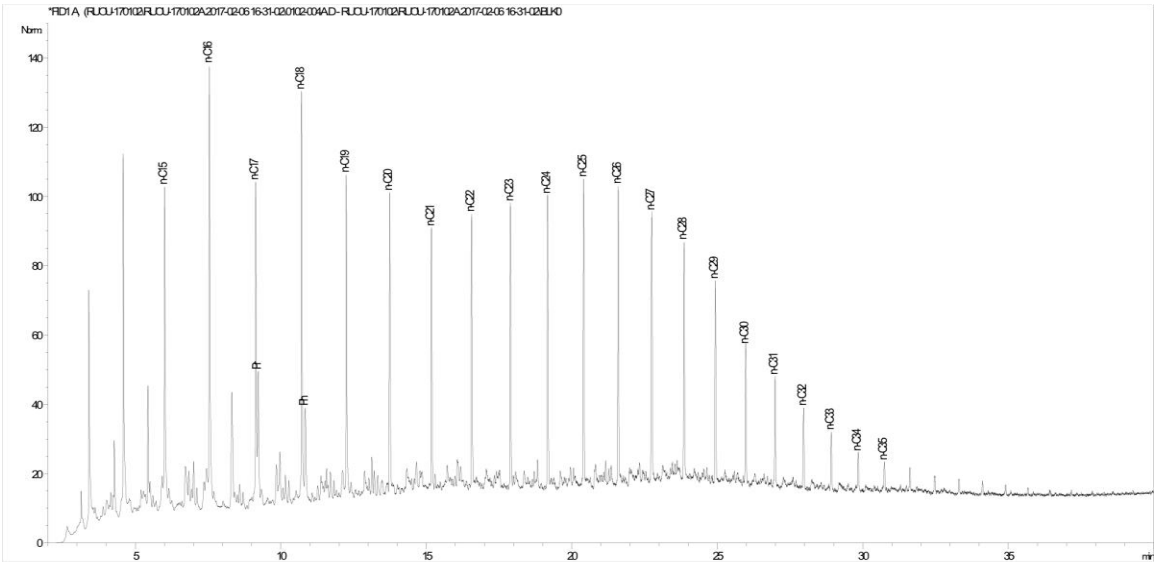

Figure 4.19: Extract GC results of the one sample from Well 3548 in Tuscarawas County and located within the oil maturity fluid window. The chromatogram shows C15 through C35 compounds, with paraffin cracking observed at about the 20-minute mark (see Section 5.3 for explanation for the loss of less than C15 compounds).

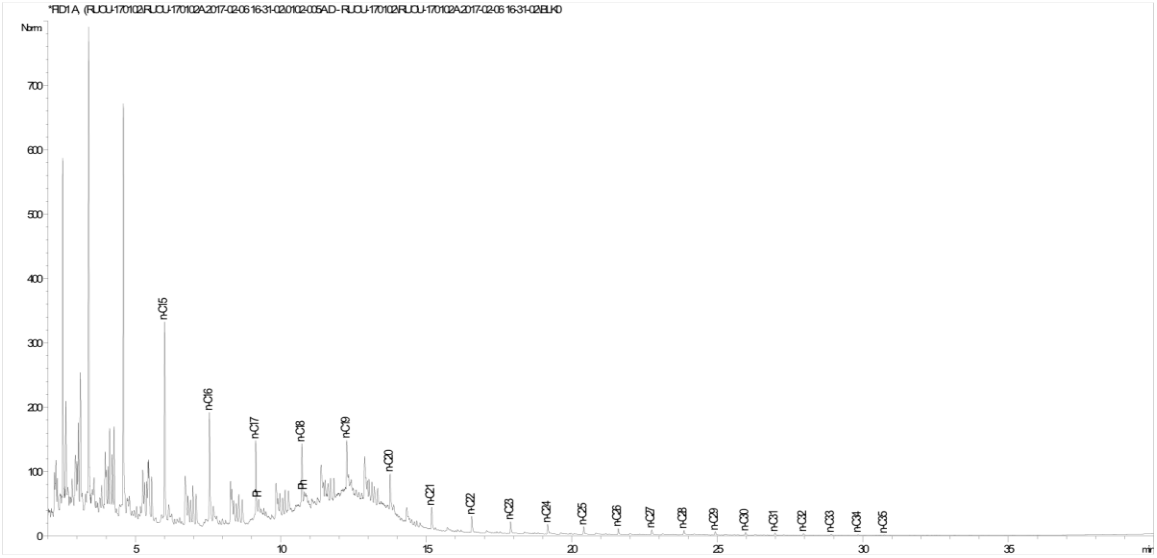

Figure 4.20: Extract GC results of one of two samples from Well 8004 in Washington County and located within the condensate maturity fluid window. Again, this chromatogram shows C15 through C35 compounds, but with increasing maturity, there is increasing light hydrocarbons, and diminishing extended alkanes (see Section 5.3 for explanation for the loss of less than C15 compounds). There is presence of cracking around the 13-minute mark, potentially a secondary cracking.

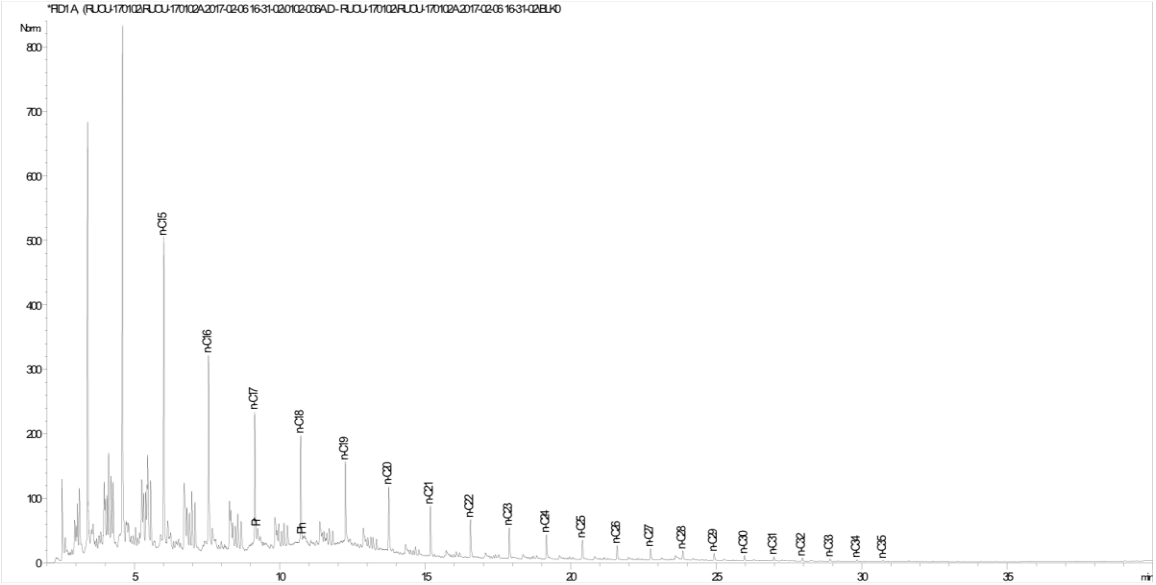

Figure 4.21: Extract GC results from the final sample from Well 8004 in Washington County and located within the condensate maturity fluid window. Likewise, this chromatogram is similar to that in Figure 4.20 in peak distribution pattern. With increasing maturity, there is increasing light hydrocarbons, and diminishing extended alkanes (see Section 5.3 for explanation for the loss of less than C15 compounds). Unlike the chromatograms from the previous maturity fluid windows, the sample from this well has much less presence of C20+ compounds.

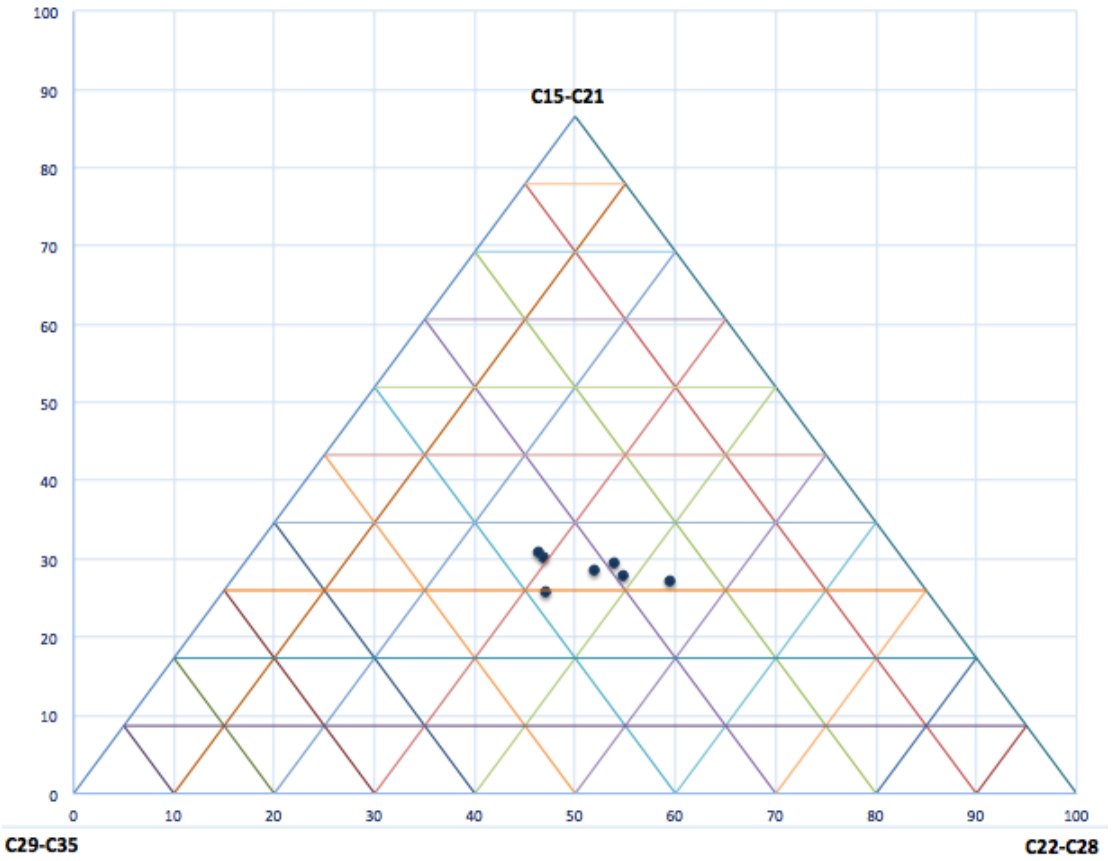

Figure 4.22: Ternary plot of (C15-C21), (C22-C28), and (C29-C35), representative of all compounds eluted during the extract GC process for all six samples. The makeup includes three samples from the low maturity fluid window (Well 3374 and 3372), one sample from the oil maturity fluid window (Well 3548), and one sample from the condensate maturity fluid window (Well 8004). As can be seen from the plot, most of the C15+ compounds are categorized according to the following: light= 30%, medium= 35%, and heavy = 35%.

CHAPTER 5

DISCUSSION

Chapter 4 discussed pertinent plots of geochemical parameters from the conventional pyrolysis method. Depth plots of TOC, S1, and S2 provided unique insights into the amount of hydrocarbons present relative to depth, amount of free oil in the samples, as well as kerogen potential. In addition to the depth plots, the chapter also presented normalized oil content plots and maximum S1 and average Tmax maps based on well locations throughout the State of Ohio. IS1 provided unique understanding into S1_1 to S1_6 signal peaks for predicting oil quality for the four wells. Ternary plots with some of the key aforementioned geochemical parameters also provided depth towards understanding oil quality within the UPP play.

This chapter provides explanations of the plots presented in the previous chapter, highlighting the key changes in results from the HAWK® Pyrolysis, Incremental S1, and Extract GC methods.

5.1. HAWK Pyrolysis

A TOC of 0.5% is generally regarded as the minimum for defining a petroleum source rock. At values greater than 1.0%, the source rock is considered to have a good petroleum generating potential. In Figure 4.1, a plot of depth versus TOC for all samples,

the wells located within the low maturity fluid window (3374 and 3372) have higher TOC values than the rest of the samples from the oil and gas fluid maturity windows. This finding is to be expected because thermal maturation is a function of depth, and the less mature a sample is (less depth and subjection to higher temperatures), the greater its potential for being a good source rock (higher TOC). Wells 3374 and 3372 are thus projected as having very good source rock potential, but with shallower depth (corresponding to low maturity), oil production from those wells is expected to yield little to no oil – the oil would be too viscous (see Table 5.1). On the other hand, Wells 3548 and 8004 are projected to have oil producing potential. The samples from these wells have greater depth (subjected to higher temperatures) and hence the lower TOC values shown on Figure 4.1.

The plot of hydrogen index versus oxygen index shown in Figure 4.2 depicts kerogen quality. Identical to the classic Van Krevelen diagram, the plot helps in discriminating the four kerogen types, Type I, II, III, and IV. Type I kerogen is highly oil-prone and designated to samples having HI values greater than 600 mgHC/gTOC, when thermally immature. Type II is oil-prone organic matter with HI values in the range of 300 to 600 mgHC/gTOC, when thermally immature. Type III is gas-prone organic matter with HI values between 50 and 200 mgHC/gTOC. Type IV kerogen is designated to inert organic matter with HI value below 50 mgHC/gTOC in thermally immature rocks (Dembicki, 2009). Based on the criteria for the various kerogen types, Wells 3374 and 3372 contain Type II kerogen, Well 3548 contains Type III kerogen, and Well 8004 contains Type III/IV kerogen. The findings are a validation to the maturity map in Figure 3.2: Well 8004 within the condensate maturity fluid window, Well 3548 within the oil

maturity fluid window, and Wells 3374 and 3372 within the low maturity fluid window.

S1 is measured in mg of hydrocarbons per gram of rock (mgHC/g of rock) and a rock with a result greater than 1mgHC/g of rock is considered to be a good source rock. Figure 4.3 is a depth versus S1 plot for all wells analyzed using the conventional pyrolysis method. Generally, free oil concentration in a rock increases with increasing depth. The reason is that at greater depths, the rock is subjected to higher temperatures (geothermal gradient) that result in the breakdown of kerogens, and subsequently conversion into free oil. As shown in Figure 4.3, samples from Well 8004 that are buried the deepest have the greatest free oil concentration. The shallowest samples are from the immature oil window. These samples are from Wells 3374 and 3372. Samples from these two wells exhibited much lower S1 concentrations than those of samples from the condensate maturity fluid window.

Figure 4.4 is a depth versus S2 plot. S2 measures the amount of hydrocarbons generated through thermal cracking of kerogen and heavy hydrocarbons. S2 also represents the existing potential of a rock to generate hydrocarbons if it were subjected to increasing burial temperatures. Measured in mgHC/g of rock, an S2 of greater than 5 mgHC/g of rock is considered to have good source rock generative potential. Kerogen yield increases with decreasing depth. The rationale is that at shallower depths, the temperature is not high enough to enable kerogen breakdown, and hence samples at these shallower depths tend to exhibit higher S2 values. When subjected to higher temperatures in situ, kerogen breakdown occurs, S2 decreases, while S1 increases. From Figure 4.4, it can be seen that samples from the low maturity fluid windows in Wells 3374 and 3372 have significantly higher S2 values than samples from the gas and oil maturity fluid

windows. Again, samples from Wells 3548 and 8004 have been subjected to higher temperatures, and have undergone kerogen breakdown, and hence are characterized by the very low S2 concentrations.

Figure 4.5 is a plot of free oil (S1) versus Tmax. Tmax, in °C, represents the temperature at which maximum generation of S2 hydrocarbons is achieved, and it is characteristic of the kerogen type and the maturity measure of the rock formation. Synonymous to the convention for depth versus S1, free oil concentration increases with increasing temperature. Higher Tmax correlates to greater depths. As seen from the plot, samples from Well 8004 stand out from the rest of the wells. This is because those samples were buried the deepest, were subjected to the highest temperatures, and have undergone the most kerogen breakdown.

The normalized oil content versus Tmax plot is shown in Figure 4.6. A normalized oil content value of less than 50 indicates low or over mature source rock, 50-100 indicates mature stained source rock, and greater than 100 indicates productive source/reservoir rock or contamination (Ruble et al. 2017). From the plot, Well 8004 clearly has more samples with normalized oil content well over 100. This result indicates that the well has highly productive reservoir rock. Conversely, samples from Wells 3374 and 3372 have normalized oil content well below 50. This finding is to be expected because Wells 3374 and 3372 are located within the low maturity fluid window (see Figure 3.2) and are projected to be less productive.

Figures 4.7 and 4.8 are maps of the State of Ohio with maximum S1 values and average Tmax values for all of the samples analyzed using the conventional pyrolysis method. In Figure 4.7, Well 8004, located within Washington County, has the highest

maximum S1 value of all the wells analyzed. Correspondingly, samples from this well were buried the deepest of all the rest, and hence have been subjected to higher temperatures and kerogen breakdown. In Figure 4.8, Well 3548 has highest average Tmax. This well is located in Tuscarawas County, and in the oil maturity fluid window (see Figure 3.2). Well 8004, located within the condensate maturity fluid window, has the second highest average Tmax, followed by Wells 3374 and 3372. Due to limited core availability for Well 3548, only 3 samples were analyzed, compared to over 40 samples each for the rest of the wells. Hence there is surprisingly higher average Tmax than samples from Well 8004.

5.2. Incremental S1

The purpose of this research is to determine the petroleum quality within the Utica-Point Pleasant formation of Ohio, using a newly developed pyrolysis method. The newly developed method, Incremental S1, enhances the bulk S1 FID signal generated during conventional pyrolysis, and generates six peaks at six different temperatures (50°C, 100°C, 150°C, 200°C, 250°C, and 300°C). The signals are designated S1_1 through S1_6, corresponding to the six different temperature settings.

The conventions used in determining the potential oil quality from any rock using the IS1 peaks are as follows: for dominant S1_1 and S1_2 signal peaks, the lighter the oil potential is; the more dominant S1_3 and S1_4 generated peaks for a sample, the more likely oil quality will be medium heavy; and finally, for dominant S1_5 and S_6 peaks for a sample, the more likely the oil quality is predicted to be heavy.

Figure 4.9 is a raw FID signal peak generated for a sample from Well 3374. As a reminder, Well 3374 is located within the low fluid maturity window, in Wyandot

County (see Figure 3.2). As can be seen on the annotated FID signals, the sample has dominant S1_6 and S1_5 peaks, and based on the convention for delineating oil quality using IS1, oil production potential, if any, for this well, would yield heavy and/or viscous oil. Figure 4.10 shows another sample from the same well. Although there are similar signal patterns as seen in Figure 4.9, there is a distinct difference between S1_6 and S1_5 peaks for this sample. The well generates peaks with dominant S1_6 and S1_5 peaks, and hence oil produced, if any, will be heavy and more viscous.

Well 3372 in Marion County, like Well 3374, is located within the low maturity fluid window (see Figure 3.2). The FID signal peaks for this sample are similar to those from Figures 4.9 and 4.10. Figure 4.11 is a generated FID signal peak for a sample from Well 3372. As can be seen from the figure, S1_6 is the predominant peak, followed by S1_5. The difference in FID signals between S1_6 and S1_5 is 0.8mv (about halfway between the differences from Figures 4.9 and 4.10). Following the same convention for wells located within the low maturity fluid window, oil from Well 3372, if any, is projected to be heavy and/or viscous.

Figure 4.12 shows results for a sample from Well 3548, located within Tuscarawas County, and falls within the oil maturity fluid window. As can be seen from the figure, the peak distribution trend is similar to the previous samples from the low maturity fluid window. With this finding, and based on the convention already established for delineating oil quality from IS1 signal peaks, Well 3548 is projected to produce medium to heavy oil.

The final well, 8004, is located in Washington County and within the condensate maturity fluid window. Figure 4.13 shows data for the first of two samples from this well.

As can be seen in Figure 4.13, S1_5 stands out as the distinct and dominant peak, followed by S1_6 (closely followed by S1_4). Unlike samples from the low and oil maturity fluid windows, peak distribution pattern is very different for samples from Well 8004. Based on the FID signal strengths, the significant S1_4 value, and using the already established convention for delineating oil quality using IS1 peaks, Well 8004 is projected to produce late light (rich/lean condensate) to medium heavy oil. Figure 4.14 is also from the same county and is also located within the condensate maturity fluid window. In this figure, the peak distribution trend is somewhat similar to that of Figure 4.13, but with a much higher FID value (6 mv compared to 4.7 mv), S1_4 signal greater than S1_6, and with a noticeable S1_3 signal peak. This suggests that Well 8004 will produce some amount of lean/rich condensate to medium quality oil. The other indication from this figure is that, although from the same well, signal peak distributions do vary, which will translate into varying oil quality at various depths/locations within the well.

The ternary plot generated from IS1 pyrolysis results is shown in Figure 4.15, and indicates that most of the petroleum fractions released at the various temperature ranges fall within 5% of light, 50% medium, and 45% heavy. The finding is to be expected because of the possible vaporization of volatiles from the condensate maturity fluid window and the presence of samples from two wells within the low maturity fluid window. At a near 50-50 split between heavy and light to medium petroleum fractions, the ternary plot highlights the possibilities of oil production within the play, depending on where drilling occurs.

So far in this section, the research has determined that low maturity fluid window samples have significantly higher S1_6 peaks compared to the other signal peaks,

samples from oil maturity fluid window generate signal patterns similar to samples from low maturity fluid window but with lower maximum FID signal, and finally, for samples within the condensate maturity fluid window, S1_5 peaks dominate the signal distributions. The ternary plot also shows the distribution of the various petroleum factions released at the different quality designations (Slight, Smedium, and Sheavy). These findings are very significant as they help in delineating potential oil quality by looking at generated IS1 signal peaks. The next section will look to validate these findings and conventions established with regard to delineating oil quality using IS1.

5.3. Extract GC

From Section 5.2, the application of IS1 in delineating oil quality presented the need for validation using an external analysis. The ternary plot in Figure 4.15 highlighted the various distributions of petroleum fraction releases at their corresponding quality designations (Slight, Smedium, Sheavy). The external analysis to help validate the IS1 convention for petroleum quality analysis is extract GC. In the ternary plot in 4.15, petroleum fractions are delineated based on boiling points (Sl = 50-100°C, Sm = 150-200°C, and Sh = 250-300°C). However, the temperature used during the GC extraction process for the samples was estimated at 300°C. This temperature setting means that although there is an acquisition of higher order saturates and aromatics (C15+), there are losses of C15- compounds. By using curve fitting of n-alkanes, the lost volatiles can be restored, and be fully accounted for (Jarvie, 2015). For the purposes of this research, C15-C21 compounds eluted during the extraction process will represent light oil potential, C22-C28 represent medium potential, and C29-C35 represent heavy potential.

The C15-C21, C22-C28, and C29-C35 designations, regardless of curve fitting, highlight the goals and/or expectations for this research.

Figure 4.16 is the first of two samples from Well 3374 in Wyandot County, located within the low maturity fluid window. GC chromatogram results for this sample show significant peak abundances for all C15+ compounds, with the highest peak being Pr. From Section 3.5, it is known that this well is located within the low maturity fluid window, and its oil production, if any, is expected to be viscous. It is also known from that same section that samples are shallower and therefore have likely not been subjected to higher temperatures, less kerogen breakdown (primary cracking), and low free oil content. The GC fingerprint in Figure 4.16 shows paraffin cracking and does validate the findings with regards to oil quality from Well 3374, with the availabilities of significantly higher C15+ peaks within the sample. Figure 4.17, the final sample within the low maturity fluid window, is also from Well 3374, and likewise, displays the same dominant C15+ compound abundances seen in Figure 4.16, with C17 being the dominant peak. The GC fingerprint for this sample also shows paraffin cracking that points to an early maturity sample.

Figure 4.18 is a sample from Well 3372, located in Marion County and within the low maturity fluid window (see Section 3.5). Although it is from the same maturity window as the previous two chromatograms, there is a very noticeable difference between the peak distributions. The chromatogram shows predominantly higher C15+ compounds, with C16 being the dominant signal, with a lower Pr signal peak, relative to the other samples from the low maturity fluid window. The presence of significant C15+ compounds and paraffin cracking at the 25-minute mark are indications of early maturity

and a very low oil quality potential from Well 3372. Likewise, samples from Well 3372 are from shallower depth, less exposure to high temperatures limiting kerogen breakdown, and hence the presence of significantly higher hydrocarbon chains.

Figure 4.19 is a sample from Well 3548, located in Tuscarawas County and within the oil maturity fluid window. Compared to chromatograms from the low maturity fluid window, this sample has relatively higher signal C15+ signal peaks but lower Pr presence. The significance of the C15+ compound presence is that it is an indication of the possibility for late medium to onset of heavy oil quality in this well. The GC fingerprint also shows paraffin cracking at the 20-minute mark, an indication of an early cracking, compared to samples from the low maturity fluid window. Only three samples were analyzed for this well due to core availability limitations. Hence the three samples are predicted (through IS1) to be from a zone of low maturity within the well, and minimal subjection to primary/kerogen cracking. Once again, the chromatogram does validate the convention already established for this well from the IS1 method; samples from this well are projected to exhibit medium to onset of heavy crude oil quality.

Figures 4.20 and 4.21 are chromatograms of two samples from Well 8004 in Washington County, and located within the condensate maturity fluid window. Of the many variations in signal distributions, the most obvious is the low signal strength for the C20+ compounds. These compounds are virtually non-existent, compared to chromatograms from the other fluid windows. Among the many possible reasons for this is that, with increasing maturity, there is an increase in light hydrocarbons, and diminishing extended alkanes, which represents the peak oil GC fingerprint (Jarvie, 2015). C15-C20 signal peaks are also significantly higher than those of the low maturity

and oil maturity fluid windows, and cracking occurs fairly sooner, at the 12-minute marks for both samples. These findings point to the convention already established by the IS1 method for samples within the condensate maturity fluid windows; samples are buried deeper and hence subjected to higher temperatures, have undergone substantial amount of primary cracking and/or kerogen breakdown resulting in more free oil concentrations, and oil quality expected to be light oil with rich/lean condensate presence (more C15- compounds upon exponential curve fitting of n-alkanes).

In order to generate a ternary plot of GC extract data similar to that of IS1, the following assumptions are made; Sl = Condensate Maturity = C15–C21 concentrations/areas, Sm = Oil Maturity = C22-C28 concentrations/areas, and Sh = Low Maturity = C29-C35 concentrations/areas.

Figure 4.22 is a ternary plot showing all C15+ compounds eluted during the extract GC process for all six samples, categorized under C15-C21 (light), C22-C28 (medium), and C29-C35 (heavy). As can be seen from the plot, most of the C15+ compounds are categorized according to the following: light = 30%, medium= 35%, and heavy = 35%. These compositions mean that the samples extracted for GC analysis have identical compositions and have not been subjected to primary (and secondary) cracking, and hence the wells have the tendency to produce medium to heavy crude, as well as lean/rich condensates.

Table 5.1 is historical production data from for the four wells that help validate the established assumptions with regards to oil quality delineation.

5.4. IS1 vs. Extract GC

In order to predict the hydrocarbon chain distributions present within a sample generated using the IS1 method, solvent extraction and GC analysis are required. Combining both results provides the visual, as well as the quantification, of hydrocarbons inherent in the research samples.

In order to resolve the relationship between IS1 and GC Extract, a plot with similar representations of analysis data is used. The plot to help relate IS1 to GC Extract is the ternary plot. Figures 4.15 and 4.22 are ternary plots for the IS1 and GC Extract methods, respectively. From Figure 4.15, it can be seen that most of the samples are categorized according to the following: Sl = 5%, Sm = 50%, and Sh = 45%. In Figure 4.22, the C15+ compound distributions are as follows: C15-C21 = 30%, C22-C27 = 35%, and C29-C35 = 35%.

Both plots indicate an almost perfect split between medium and heavy oil quality, and thus help in relating IS1 to GC Extract in predicting oil quality from any rock.

Table 5.1 – Historical Production Data for the Researched Wells. The table validates the conventions established with the IS1 method through the production numbers associated with each well. Low maturity fluid windows did not produce any oil, whereas oil and condensate maturity wells produced some amount of oil (DrillingInfo, 2017).

API#	Core #	Fluid Maturity Window	County	Depth	Cum. Oil
				ft	bbl
34-175-202870000	3374	Low	Wyandot	2052	0
34-101-201960000	3372	Low	Marion	2204	0
34-157-253340000	3548	Oil	Tuscarawas	8700	4,729
34-167-297200100	8004	Condensate	Washington	14893	526

CHAPTER 6

FURTHER WORK

The goal of the research was to understand the application of IS1 in determining the potential oil quality inherent in any source or reservoir rock. The IS1 method is inexpensive, less time-consuming, and provides an enhancement into the divisions within a generated S1 signal using the conventional pyrolysis method. In its extended applications, S1 can be used to predict the API gravity of any rock. Together with extract GC, the method is capable of predicting and quantifying oil quality within any source or reservoir rock.

6.1. Conclusions

The work done in this research covered four counties, Wyandot, Marion, Tuscarawas, and Washington, in the State of Ohio. The four wells studied in the research are from the four counties. The initial phase of conducting HAWK® pyrolysis on the 190 samples helped in establishing a baseline for S1 potential for the wells, as well as understanding the area of fluid windows. IS1 then helped screen the windows for oil quality for subsamples with initial S1 values greater or equal to 1 mgHC/grock.

Solvent extraction and GC analysis aided in quantifying the carbon numbers and understanding the hydrocarbon chains within each well. Combining IS1 and extract GC

methods, understanding the quality of oil within the four wells, comprising low maturity, oil maturity, and condensate maturity windows, is possible.

In conclusion, the newly developed analytical method, Incremental S1, is capable of predicting the quality of oil within a reservoir or a source rock; however, the volatilization of short hydrocarbon chains and the cracking of longer hydrocarbon chains add ambiguity to the interpretation. Because of this ambiguity, the interpreter must carefully analyze the data before reaching a conclusion on oil quality analysis using the Incremental S1 pyrolysis method.

6.2. Suggestions on Future Work

- Increase core sampling across the various fluid maturity windows.
- Research into how to accurately account for the volatilized carbon chains during the IS1 analysis, as well as during the GC Extraction process.
- Test the limits of IS1, if any, in its application to samples within the condensate maturity fluid window.
- Apply IS1 to other unconventional shale plays across the nation to maximize its applications.
- Build enough libraries of IS1 analysis to aid in predicting oil quality without the need for solvent extraction and GC analysis.

APPENDIX A

HAWK PYROLYSIS DATA: CORE #3372

Table A.1: Detailed Conventional Pyrolysis Data for Core #3372 (API: 34-101-201960000)

API # (Core #)	Sample ID	Depth	Tmax (°C)	Weight (mg)	S1 mgHC/g rock)	S2 (mgHC/g rock)	S3 (mgCO2/g rock)	TOC (%)
34-101-201960000 (3372)	EGI.Nov.2016.00334	1316 ft	431	74.6	0.46	8.92	0.25	3.98
	EGI.Nov.2016.00335	1302 ft	429	71.3	0.56	11.08	0.5	4.12
	EGI.Nov.2016.00336	1296 ft	434	73.1	0.27	4.59	0.35	4.37
	EGI.Nov.2016.00337	1242 ft	429	75.7	0.61	12.43	0.43	4.55
	EGI.Nov.2016.00338	1300 ft	433	74.9	0.32	5.54	0.36	4.08
	EGI.Nov.2016.00339	1250 ft	428	74.1	0.71	14.27	0.67	4.3
	EGI.Nov.2016.00340	1262 ft	430	71.3	0.69	14.45	0.42	5.19
	EGI.Nov.2016.00341	1338 ft	428	76.4	0.73	15.1	0.52	5.21
	EGI.Nov.2016.00342	1298 ft	432	74.4	0.31	5.01	0.4	3.53
	EGI.Nov.2016.00343	1240 ft	429	71.5	0.62	12.36	0.57	5.24
	EGI.Nov.2016.00344	1246 ft	430	75.4	0.62	12.72	0.45	4.21
	EGI.Nov.2016.00345	1314 ft	433	78.8	0.38	6.63	0.39	3.53
	EGI.Nov.2016.00346	1248 ft	428	73.7	0.78	16.45	0.38	5.24
	EGI.Nov.2016.00347	1318 ft	432	72.7	0.39	7.29	0.37	3.24
	EGI.Nov.2016.00348	1252 ft	429	76.3	0.81	17	0.3	4.43
	EGI.Nov.2016.00349	1286 ft	430	78.5	0.76	16.13	0.3	4.09
	EGI.Nov.2016.00350	1270 ft	428	72.9	0.77	16.01	0.47	4.87
	EGI.Nov.2016.00351	1284 ft	430	77.2	0.49	9.24	0.38	4.23
	EGI.Nov.2016.00352	1360 ft	431	72.7	0.5	7.96	0.64	3.78
	EGI.Nov.2016.00353	1350 ft	432	79.6	0.48	7.86	0.53	5.71

Table A.1 Continued

API # (Core #)	Sample ID	Depth	Tmax (°C)	Weight (mg)	S1 mgHC/g rock)	S2 (mgHC/g rock)	S3 (mgCO2/g rock)	TOC (%)
34-101-20196000 0 (3372)	EGI.Nov.2016.00354	1324 ft	429	74.8	0.62	12.9	0.45	4.66
	EGI.Nov.2016.00355	1336 ft	427	73.3	0.93	18.95	0.5	4.97
	EGI.Nov.2016.00356	1254 ft	432	73.8	0.07	0.37	0.76	3.68
	EGI.Nov.2016.00357	1288 ft	431	75.5	0.49	9.69	0.47	5.08
	EGI.Nov.2016.00358	1294 ft	432	73.8	0.4	7.4	0.41	4.44
	EGI.Nov.2016.00359	1310 ft	430	78.3	0.51	10.62	0.57	3.97
	EGI.Nov.2016.00360	1308 ft	430	72.5	0.57	11.84	0.46	5.16
	EGI.Nov.2016.00361	1282 ft	428	76.9	0.89	19.98	0.39	4.74
	EGI.Nov.2016.00362	1334 ft	428	71.2	0.82	16.32	0.39	6.07
	EGI.Nov.2016.00363	1268 ft	427	70.2	1.13	24.06	0.45	6.16
	EGI.Nov.2016.00364	1322 ft	430	74.5	0.52	9.94	0.39	3.07
	EGI.Nov.2016.00365	1260 ft	429	70.6	0.62	11.82	0.34	4.34
	EGI.Nov.2016.00366	1258 ft	429	73.8	0.65	12.76	0.45	5.04
	EGI.Nov.2016.00367	1244 ft	429	75	0.71	14.35	0.52	5.17
	EGI.Nov.2016.00368	1326 ft	429	70.1	0.56	11	0.46	3.18
	EGI.Nov.2016.00369	1276 ft	430	75.6	0.62	12.49	0.45	5.06
	EGI.Nov.2016.00370	1358 ft	433	76.2	0.33	5.06	0.37	3.24
	EGI.Nov.2016.00371	1274 ft	429	77.5	0.79	17.22	0.47	4.4
	EGI.Nov.2016.00372	1256 ft	429	71.4	0.82	18.03	0.36	4.59
	EGI.Nov.2016.00373	1320 ft	432	74.1	0.39	6.42	0.38	3.39

Table A.1 Continued

API #	Sample ID	Depth	Tmax (°C)	Weight (mg)	S1 mgHC/g rock)	S2 (mgHC/g rock)	S3 (mgCO2/g rock)	TOC (%)
34-101-20196000 0 (3372)	EGI.Nov.2016.00374	1328 ft	429	74.4	0.7	14.35	0.34	6.58
	EGI.Nov.2016.00375	1348 ft	432	74.9	0.53	5.47	0.37	3.04
	EGI.Nov.2016.00376	1340 ft	430	75.2	0.65	12.12	0.35	3.66
	EGI.Nov.2016.00377	1272 ft	429	74.9	0.65	12.79	0.25	3.82
	EGI.Nov.2016.00378	1304 ft	433	75.8	0.3	5.15	0.3	4.35
	EGI.Nov.2016.00379	1332 ft	429	76.7	0.64	13.18	0.34	3.47
	EGI.Nov.2016.00380	1280 ft	430	77.2	0.74	17.06	0.33	4.98
	EGI.Nov.2016.00381	1290 ft	429	74.8	0.62	12.86	0.42	4.83
	EGI.Nov.2016.00382	1356 ft	433	74	0.39	4.72	0.24	3.48
	EGI.Nov.2016.00383	1312 ft	431	73.3	0.41	7.92	0.42	3.78
	EGI.Nov.2016.00384	1278 ft	431	78.7	0.63	13.19	0.26	4.38
	EGI.Nov.2016.00385	1292 ft	431	77.3	0.45	8.75	0.31	3.1
	EGI.Nov.2016.00386	1342 ft	429	77.6	0.64	13.04	0.39	3.78
	EGI.Nov.2016.00387	1354 ft	433	71.7	0.34	4.84	0.41	4.95
	EGI.Nov.2016.00388	1346 ft	433	74.4	0.41	5.06	0.47	3.66
	EGI.Nov.2016.00389	1266 ft	428	73.8	0.7	14.21	0.32	5.49
	EGI.Nov.2016.00390	1330 ft	427	77	0.93	19.35	0.58	5.09
	EGI.Nov.2016.00391	1264 ft	429	71.1	0.78	15.95	0.27	6.13
	EGI.Nov.2016.00392	1354 ft	430	77.6	0.48	8.09	0.33	4.91
	EGI.Nov.2016.00393	1344 ft	427	73.6	0.87	18.27	0.31	4.79

APPENDIX B

HAWK PYROLYSIS DATA: CORE #3374

Table B.1: Detailed Conventional Pyrolysis Data for Core #3374 (API: 34-175-202870000)

API # (Core #)	Sample ID	Depth	Tmax (°C)	Weight (mg)	S1 mgHC/g rock)	S2 (mgHC/g rock)	S3 (mgCO2/g rock)	TOC (%)
34-175-20287000 0 (3374)	EGI.Nov.2016.00293	1178 ft	430	78.6	0.98	16.93	0.32	3.37
	EGI.Nov.2016.00294	1160 ft	430	70.8	0.79	13.1	0.43	3
	EGI.Nov.2016.00295	1202 ft	431	74.9	0.58	8.38	0.56	2.39
	EGI.Nov.2016.00296	1176 ft	432	73.2	0.47	6.57	0.54	2.29
	EGI.Nov.2016.00297	1220 ft	430	73.8	0.48	6.06	0.35	1.87
	EGI.Nov.2016.00298	1198 ft	433	78.9	0.34	4	0.39	2.39
	EGI.Nov.2016.00299	1218 ft	431	78.6	0.55	7.92	0.2	2.38
	EGI.Nov.2016.00300	1180 ft	431	71	0.98	17.05	0.3	3.13
	EGI.Nov.2016.00301	1188 ft	432	73.9	0.78	13.45	0.51	3.09
	EGI.Nov.2016.00302	1216 ft	434	72.5	0.41	5.64	0.41	2.16

Table B.1 Continued

API #	Sample ID	Depth	Tmax (°C)	Weight (mg)	S1 mgHC/g rock)	S2 (mgHC/g rock)	S3 (mgCO2/g rock)	TOC (%)
34-175-20287000000 (33744)	EGI.Nov.2016.00303	1238 ft	431	79.2	0.51	7.28	0.49	1.97
	EGI.Nov.2016.00304	1184 ft	430	72	0.86	13.76	0.35	2.85
	EGI.Nov.2016.00305	1186 ft	430	74.5	0.94	15.45	0.33	3.36
	EGI.Nov.2016.00306	1228 ft	430	76.4	0.72	11.62	0.45	2.45
	EGI.Nov.2016.00307	1172 ft	431	72.3	0.98	16.53	0.38	3.59
	EGI.Nov.2016.00308	1236 ft	432	69.1	0.36	4.23	0.49	2.5
	EGI.Nov.2016.00309	1230 ft	434	69.8	0.36	5.03	0.45	2.56
	EGI.Nov.2016.00310	1232 ft	435	72.6	0.17	1.58	0.35	1.72
	EGI.Nov.2016.00311	1214 ft	433	76.3	0.47	6.33	0.5	2.87
	EGI.Nov.2016.00312	1226 ft	430	77.1	0.7	10.7	0.27	2.05
	EGI.Nov.2016.00313	1224 ft	430	72.7	0.42	5.37	0.7	2.31
	EGI.Nov.2016.00314	1240 ft	433	74.3	0.35	5.07	0.46	2
	EGI.Nov.2016.00315	1162 ft	431	76.5	0.69	10.73	0.44	2.98
	EGI.Nov.2016.00316	1170 ft	430	70.5	1.16	20.66	0.37	3.86
	EGI.Nov.2016.00317	1204 ft	432	75.6	0.5	6.74	0.36	1.98
	EGI.Nov.2016.00318	1164 ft	432	75.8	0.65	10.24	0.43	2.84
	EGI.Nov.2016.00319	1222 ft	432	69.8	0.41	5.08	0.51	2.12
	EGI.Nov.2016.00320	1210 ft	431	70.3	0.55	7.71	0.37	2.32
	EGI.Nov.2016.00321	1234 ft	430	72.8	0.62	9.26	0.41	2.49
	EGI.Nov.2016.00322	1190 ft	430	73.7	0.75	11.61	0.34	2.41
	EGI.Nov.2016.00323	1206 ft	433	72	0.51	7.72	0.61	2.34
	EGI.Nov.2016.00324	1212 ft	430	78	0.66	10.3	0.34	2.59
	EGI.Nov.2016.00325	1182 ft	432	70.8	0.58	9.04	0.48	2.12
	EGI.Nov.2016.00326	1192 ft	432	75.4	0.7	11.29	0.37	2.42
	EGI.Nov.2016.00327	1208 ft	432	73.2	0.52	7.44	0.48	2.37
	EGI.Nov.2016.00328	1174 ft	429	70.5	1.04	16.93	0.43	6.39
	EGI.Nov.2016.00329	1200 ft	431	71.5	0.58	7.72	0.41	3.99
	EGI.Nov.2016.00330	1166 ft	431	74.2	1.23	20.04	0.38	7.23
	EGI.Nov.2016.00331	1196 ft	433	71.7	0.64	10.99	0.32	4.69
	EGI.Nov.2016.00332	1194 ft	432	76.1	0.66	9.71	0.37	4.98
	EGI.Nov.2016.00333	1168 ft	428	75.3	1.45	24.02	0.23	6.05

APPENDIX C

HAWK PYROLYSIS DATA: CORE #3548

Table C.1: Detailed Conventional Pyrolysis Data for Core #3548 (API: 34-157-253340000)

API # (Core #)	Sample ID	Depth	Tmax (°C)	Weight (mg)	S1 mgHC/g rock)	S2 (mgHC/g rock)	S3 (mg CO2/g rock)	TOC (%)
34-157-25334000 (3548)	EGI.Nov.2016.00198	6141 ft	446	71.8	0.64	2.94	0.54	2.3
	EGI.Nov.2016.00199	6282 ft	448	77.1	0.89	2.52	0.42	4.65
	EGI.Nov.2016.00200	6336 ft	453	78.1	1.06	4.63	0.44	3.3

APPENDIX D

HAWK PYROLYSIS DATA: CORE #8004

Table D.1: Detailed Conventional Pyrolysis Data for Core #8004 (API: 34-167-297200100)

API # (Core #)	Sample ID	Depth	Tmax (°C)	Weight (mg)	S1 mgHC/g rock)	S2 (mg HC/g rock)	S3 (mg CO2/g rock)	TOC (%)
34-167-29720010 0 (8004)	EGI.Nov.2016.00201	7986 ft	421	72.4	0.17	0.18	0.25	2.21
	EGI.Nov.2016.00202	7976 ft	348	77.7	0.37	0.31	0.22	2.86
	EGI.Nov.2016.00203	7944 ft	472	71.8	0.36	0.23	0.56	3.04
	EGI.Nov.2016.00204	7916 ft	471	72.3	1.19	0.56	0.53	2.32
	EGI.Nov.2016.00205	7936 ft	480	73.9	1.37	0.47	0.48	2.53
	EGI.Nov.2016.00206	7892 ft	474	73.9	1.48	1.06	0.46	2.94
	EGI.Nov.2016.00207	7974 ft	327	72.8	0.23	0.17	0.36	1.98
	EGI.Nov.2016.00208	7874 ft	464	69.4	1.92	0.99	0.5	2.91
	EGI.Nov.2016.00209	7890 ft	478	73.2	1.02	0.99	0.45	2.6
	EGI.Nov.2016.00210	7980 ft	466	69	0.25	0.18	0.48	3.72

Table D.1 Continued

API # (Core #)	Sample ID	Depth	Tmax (°C)	Weight (mg)	S1 mgHC/g rock)	S2 (mgHC/g rock)	S3 (mgCO2/g rock)	TOC (%)
34-167-29720010 00 (8004)	EGI.Nov.2016.00211	7970 ft	338	76.8	0.16	0.17	0.42	2.35
	EGI.Nov.2016.00212	7884 ft	475	79.7	1.22	1.03	0.46	1.94
	EGI.Nov.2016.00213	7886 ft	475	78	0.88	0.87	0.43	2.25
	EGI.Nov.2016.00214	7926 ft	415	71.6	0.1	0.16	0.44	4.16
	EGI.Nov.2016.00215	7940 ft	478	74.6	1.12	0.58	0.38	2.77
	EGI.Nov.2016.00216	7946 ft	488	76.5	0.78	0.67	0.51	2.49
	EGI.Nov.2016.00217	7962 ft	490	74.7	0.27	0.34	0.37	2.12
	EGI.Nov.2016.00218	7922 ft	482	68.4	3.08	1.72	0.36	2.59
	EGI.Nov.2016.00219	7956 ft	454	78.1	0.62	0.24	0.37	2.89
	EGI.Nov.2016.00220	7910 ft	477	72.1	2.24	1.04	0.39	2.79
	EGI.Nov.2016.00221	7958 ft	506	74	0.17	0.16	0.48	3.68
	EGI.Nov.2016.00222	7904 ft	477	67.5	3.32	1.36	0.37	2.89
	EGI.Nov.2016.00223	7928 ft	474	79.4	0.18	0.17	0.22	2.61
	EGI.Nov.2016.00224	7903 ft	475	75.9	2.03	1.2	0.25	1.75
	EGI.Nov.2016.00225	7964 ft	417	75.1	0.1	0.16	0.52	2.32
	EGI.Nov.2016.00226	7938 ft	490	74.9	0.79	0.83	0.39	2.37
	EGI.Nov.2016.00227	7898 ft	470	72.4	2.59	1.1	0.49	3.44
	EGI.Nov.2016.00228	7878 ft	468	69.2	1.29	0.91	0.37	4.09
	EGI.Nov.2016.00229	7896 ft	481	77.9	2.73	1.29	0.19	2.84
	EGI.Nov.2016.00230	7880 ft	473	69.5	1.22	1.04	0.34	3.21

Table D.1 Continued

API # (Core #)	Sample ID	Depth	Tmax (°C)	Weight (mg)	S1 mgHC/g rock)	S2 (mgHC/g rock)	S3 (mgCO2/g rock)	TOC (%)
34-167-29720010 0 (8004)	EGI.Nov.2016.00231	7882 ft	474	67.5	1.17	0.9	0.39	2.82
	EGI.Nov.2016.00232	7950 ft	479	75.8	1.36	0.87	0.47	2.26
	EGI.Nov.2016.00233	7934 ft	456	76.2	0.34	0.23	0.44	2.31
	EGI.Nov.2016.00234	7920 ft	473	77.8	2.38	1.3	0.36	2.46
	EGI.Nov.2016.00235	7984 ft	428	78.2	0.07	0.14	0.54	2.34
	EGI.Nov.2016.00236	7930 ft	499	68.4	0.34	0.22	0.27	1.8
	EGI.Nov.2016.00237	7968 ft	477	73.2	0.11	0.15	0.42	2.91
	EGI.Nov.2016.00238	7914 ft	479	69.4	1.36	1.15	0.41	3.18
	EGI.Nov.2016.00239	7998 ft	522	71.5	0.17	0.24	0.52	3.2
	EGI.Nov.2016.00240	7902 ft	467	73.8	3.15	1.02	0.42	2.74
	EGI.Nov.2016.00242	7982 ft	423	71.3	0.09	0.16	0.45	3.06
	EGI.Nov.2016.00243	7952 ft	477	67.2	1.12	0.77	0.65	2.71
	EGI.Nov.2016.00244	7996 ft	313	71.7	0.32	0.31	0.53	2.49
	EGI.Nov.2016.00245	7799.5 ft	335	72.2	0.18	0.2	0.44	2.62
	EGI.Nov.2016.00246	7805.75 ft	317	74.8	0.14	0.18	0.34	2.18
	EGI.Nov.2016.00247	7851.75 ft	476	72.3	0.36	0.37	0.59	3.04
	EGI.Nov.2016.00248	7869.75 ft	472	76.4	1.5	1	0.48	3.37
	EGI.Nov.2016.00249	7925.45 ft	477	71	0.55	0.3	0.43	2.32
	EGI.Nov.2016.00250	7784 ft	312	71.7	0.4	0.28	0.4	2.3
	EGI.Nov.2016.00251	7854 ft	479	70.8	0.33	0.36	0.4	3.32

Table D.1 Continued

API # (Core #)	Sample ID	Depth	Tmax (°C)	Weight (mg)	S1 mgHC/g rock)	S2 (mg HC/g rock)	S3 (mgCO2/g rock)	TOC (%)
34-167-29720010 0 (8004)	EGI.Nov.2016.00252	7790 ft	323	77.3	0.58	0.38	0.24	2.29
	EGI.Nov.2016.00253	7788 ft	315	73.1	0.41	0.37	0.55	3.31
	EGI.Nov.2016.00254	7818 ft	317	75.9	0.14	0.23	0.36	2.62
	EGI.Nov.2016.00255	7820 ft	623	71.2	0.09	0.18	0.49	2.69
	EGI.Nov.2016.00256	7861.95 ft	467	77	0.95	0.65	0.2	2.79
	EGI.Nov.2016.00257	7782 ft	321	72.3	0.36	0.36	0.5	3.63
	EGI.Nov.2016.00258	7850 ft	497	76.6	0.31	0.44	0.31	2.99
	EGI.Nov.2016.00259	7844 ft	495	70.9	0.45	0.42	0.51	2.88
	EGI.Nov.2016.00260	7794 ft	419	70.4	0.27	0.25	0.42	3.31
	EGI.Nov.2016.00261	7798 ft	319	73.1	0.44	0.33	0.48	2.24
	EGI.Nov.2016.00262	7806 ft	513	76	0.05	0.17	0.32	2.76
	EGI.Nov.2016.00263	7828 ft	319	79.2	0.24	0.33	0.34	1.7
	EGI.Nov.2016.00264	7848 ft	481	71.8	0.15	0.26	0.42	1.86
	EGI.Nov.2016.00265	7830 ft	502	71.3	0.16	0.26	0.67	2.03
	EGI.Nov.2016.00266	7812 ft	320	70.5	0.11	0.23	0.48	1.94
	EGI.Nov.2016.00267	7804 ft	419	77.6	0.25	0.21	0.28	1.79
	EGI.Nov.2016.00268	7832 ft	475	68.2	0.32	0.36	0.52	2.13
	EGI.Nov.2016.00269	7834 ft	506	75.6	0.09	0.22	0.44	2.04
	EGI.Nov.2016.00270	7800 ft	322	69.1	0.39	0.37	0.37	1.47
	EGI.Nov.2016.00271	7814 ft	337	72.7	0.29	0.24	0.42	2.02

Table D.1 Continued

API # (Core #)	Sample ID	Depth	Tmax (°C)	Weight (mg)	S1 mgHC/g rock)	S2 (mgHC/g rock)	S3 (mgCO2/g rock)	TOC (%)
34-167-29720010080 04)	EGI.Nov.2016.00272	7802 ft	316	72.6	0.16	0.26	0.41	1.87
	EGI.Nov.2016.00273	7796 ft	325	77.2	0.14	0.24	0.37	1.23
	EGI.Nov.2016.00274	7792 ft	320	70.6	0.43	0.31	0.37	1.66
	EGI.Nov.2016.00275	7842 ft	318	74.8	0.24	0.29	0.33	1.64
	EGI.Nov.2016.00276	7808 ft	316	72.2	0.23	0.26	0.54	1.8
	EGI.Nov.2016.00277	7810 ft	314	72.4	0.18	0.24	0.37	1.89
	EGI.Nov.2016.00278	7826 ft	426	71.1	0.13	0.2	0.36	1.98
	EGI.Nov.2016.00279	7858 ft	473	75.5	0.52	0.62	0.36	1.65
	EGI.Nov.2016.00280	7870 ft	468	68.7	0.95	1.03	0.57	1.8
	EGI.Nov.2016.00281	7824 ft	492	74	0.17	0.28	0.59	1.79
	EGI.Nov.2016.00282	7856 ft	474	73.8	0.74	0.56	0.28	1.95
	EGI.Nov.2016.00283	7822 ft	319	70.9	0.1	0.22	0.31	1.99
	EGI.Nov.2016.00284	7872 ft	473	75.4	0.58	0.71	0.35	1.57
	EGI.Nov.2016.00285	7860 ft	468	70.8	1.05	0.55	0.46	1.89
	EGI.Nov.2016.00286	7840 ft	485	72.4	0.14	0.24	0.37	2.1
	EGI.Nov.2016.00287	7864 ft	469	73.6	0.67	0.63	0.24	1.86
	EGI.Nov.2016.00288	7866 ft	469	74	1.78	1.07	0.28	1.39
	EGI.Nov.2016.00289	7836 ft	330	71.6	0.29	0.27	0.49	1.83
	EGI.Nov.2016.00290	7868 ft	471	71.1	0.73	0.95	0.3	1.61
	EGI.Nov.2016.00291	7852 ft	470	76.2	2.86	1.3	0.32	1.55
	EGI.Nov.2016.00292	7838 ft	316	69.8	0.25	0.27	0.43	1.81

APPENDIX E

DATA COMPARING IS1 SIGNAL PEAKS

Table E.1: A Summary of S1 Values for all 31 Samples Using the Incremental S1 (IS1) Method.

Incremental S1 (mg HC/g rock)						
Sample ID	S1_1	S1_2	S1_3	S1_4	S1_5	S1_6
EGI.Nov.2016.00200	0.00536	0.01565	0.08397	0.18627	0.29195	0.35091
EGI.Nov.2016.00204	0.00451	0.07266	0.33088	0.45116	0.31087	0.15144
EGI.Nov.2016.00205	0.00395	0.08017	0.46678	0.58787	0.32163	0.14361
EGI.Nov.2016.00206	0.00254	0.07699	0.34326	0.47138	0.45831	0.29102
EGI.Nov.2016.00208	0.00428	0.1014	0.43762	0.66053	0.54793	0.30628
EGI.Nov.2016.00209	0.00505	0.0288	0.14556	0.27464	0.32167	0.23293
EGI.Nov.2016.00215	0.00434	0.05063	0.23467	0.40167	0.33728	0.1918
EGI.Nov.2016.00218	0.00415	0.1377	0.6464	1.03933	0.99801	0.61527
EGI.Nov.2016.00220	0.00369	0.15165	0.60253	0.81753	0.64858	0.38092
EGI.Nov.2016.00212	0.00548	0.04745	0.22777	0.36776	0.3845	0.26951
EGI.Nov.2016.00222	0.00312	0.22891	1.0403	1.3305	0.98556	0.53512
EGI.Nov.2016.00224	0.00343	0.13111	0.54129	0.74896	0.66644	0.40687

Table E.1 Continued						
Incremental S1 (mg HC/g rock)						
Sample ID	S1_1	S1_2	S1_3	S1_4	S1_5	S1_6
EGI.Nov.2016.00227	0.00238	0.20681	0.78321	0.99284	0.813	0.45753
EGI.Nov.2016.00228	0.00314	0.05754	0.26488	0.44844	0.4428	0.27898
EGI.Nov.2016.00229	0.00417	0.1842	0.7436	1.0329	0.82539	0.46397
EGI.Nov.2016.00230	0.00443	0.08574	0.36487	0.50946	0.46795	0.29171
EGI.Nov.2016.00231	0.00475	0.0604	0.26941	0.44809	0.4349	0.271
EGI.Nov.2016.00232	0.00523	0.0535	0.24213	0.47719	0.51181	0.32294
EGI.Nov.2016.00234	0.00416	0.14769	0.6295	0.92353	0.85099	0.54381
EGI.Nov.2016.00238	0.00495	0.10276	0.4041	0.5327	0.48618	0.30512
EGI.Nov.2016.00240	0.00461	0.23634	1.11673	1.43148	0.96058	0.46867
EGI.Nov.2016.00243	0.0025	0.0476	0.23865	0.39838	0.42506	0.26573
EGI.Nov.2016.00248	0.00464	0.06461	0.34972	0.54125	0.50339	0.31799
EGI.Nov.2016.00285	0.00514	0.07205	0.35641	0.48936	0.34006	0.17486
EGI.Nov.2016.00288	0.00492	0.08315	0.42976	0.72871	0.62066	0.3441
EGI.Nov.2016.00291	0.12205	0.32695	1.03701	1.36382	1.08345	0.68233
EGI.Nov.2016.00316	0.00559	0.08137	0.26628	0.36942	0.38287	0.42832
EGI.Nov.2016.00328	0.00223	0.06213	0.2074	0.30405	0.32434	0.37474
EGI.Nov.2016.00330	0.00567	0.06795	0.22878	0.34549	0.4061	0.48126
EGI.Nov.2016.00333	0.00703	0.08026	0.27665	0.40788	0.45749	0.52545
EGI.Nov.2016.00363	0.00467	0.06566	0.21952	0.31747	0.35677	0.43455

Table E.2: IS1 Experimental Data for Ternary Plot

Sample ID	Sl (50°C+100°C)	Sh (250°C+300°C)	Sm (150°C+200°C)
EGI.Nov.2016.00316	0.056691	0.528864	0.414445
EGI.Nov.2016.00328	0.050481	0.548345	0.401174
EGI.Nov.2016.00330	0.047952	0.577991	0.374057
EGI.Nov.2016.00333	0.049741	0.560157	0.390102
EGI.Nov.2016.00363	0.050284	0.565781	0.383935
EGI.Nov.2016.00200	0.022491	0.688205	0.289304
EGI.Nov.2016.00204	0.058395	0.349836	0.591769
EGI.Nov.2016.00205	0.052444	0.290046	0.657510
EGI.Nov.2016.00206	0.048396	0.455936	0.495668
EGI.Nov.2016.00208	0.051350	0.415059	0.533590

Table E.2 Continued			
Sample ID	Sl (50°C+100°C)	Sh (250°C+300°C)	Sm (150°C+200°C)
EGI.Nov.2016.00209	0.033561	0.549839	0.416600
EGI.Nov.2016.00215	0.045040	0.433533	0.521426
EGI.Nov.2016.00218	0.041225	0.468860	0.489915
EGI.Nov.2016.00220	0.059632	0.395218	0.545150
EGI.Nov.2016.00212	0.040637	0.502132	0.457230
EGI.Nov.2016.00222	0.056269	0.368784	0.574947
EGI.Nov.2016.00224	0.053857	0.429651	0.516492
EGI.Nov.2016.00227	0.064254	0.390239	0.545507
EGI.Nov.2016.00228	0.040570	0.482541	0.476889
EGI.Nov.2016.00229	0.057884	0.396212	0.545904
EGI.Nov.2016.00230	0.052298	0.440600	0.507102
EGI.Nov.2016.00231	0.043769	0.474219	0.482012
EGI.Nov.2016.00232	0.036414	0.517577	0.446008
EGI.Nov.2016.00234	0.048989	0.449981	0.501029
EGI.Nov.2016.00238	0.058672	0.431037	0.510290
EGI.Nov.2016.00240	0.057118	0.338813	0.604069
EGI.Nov.2016.00243	0.036355	0.501329	0.462316
EGI.Nov.2016.00248	0.038873	0.461032	0.500095

APPENDIX F

EXTRACT GC DATA FOR TERNARY PLOT

Table F.1: GC Extract Data for Ternary Plot

C15-C21	C29-C35	C22-C28
35.77993	35.83401	28.38606
34.73152	35.80951	29.45897
29.78727	38.10973	32.10300
34.07634	29.07683	36.84683
32.96262	31.64588	35.39149
32.12355	29.23850	38.63795
31.52501	24.84302	43.63197

APPENDIX G

HC VS. TIME: IS1 PEAKS

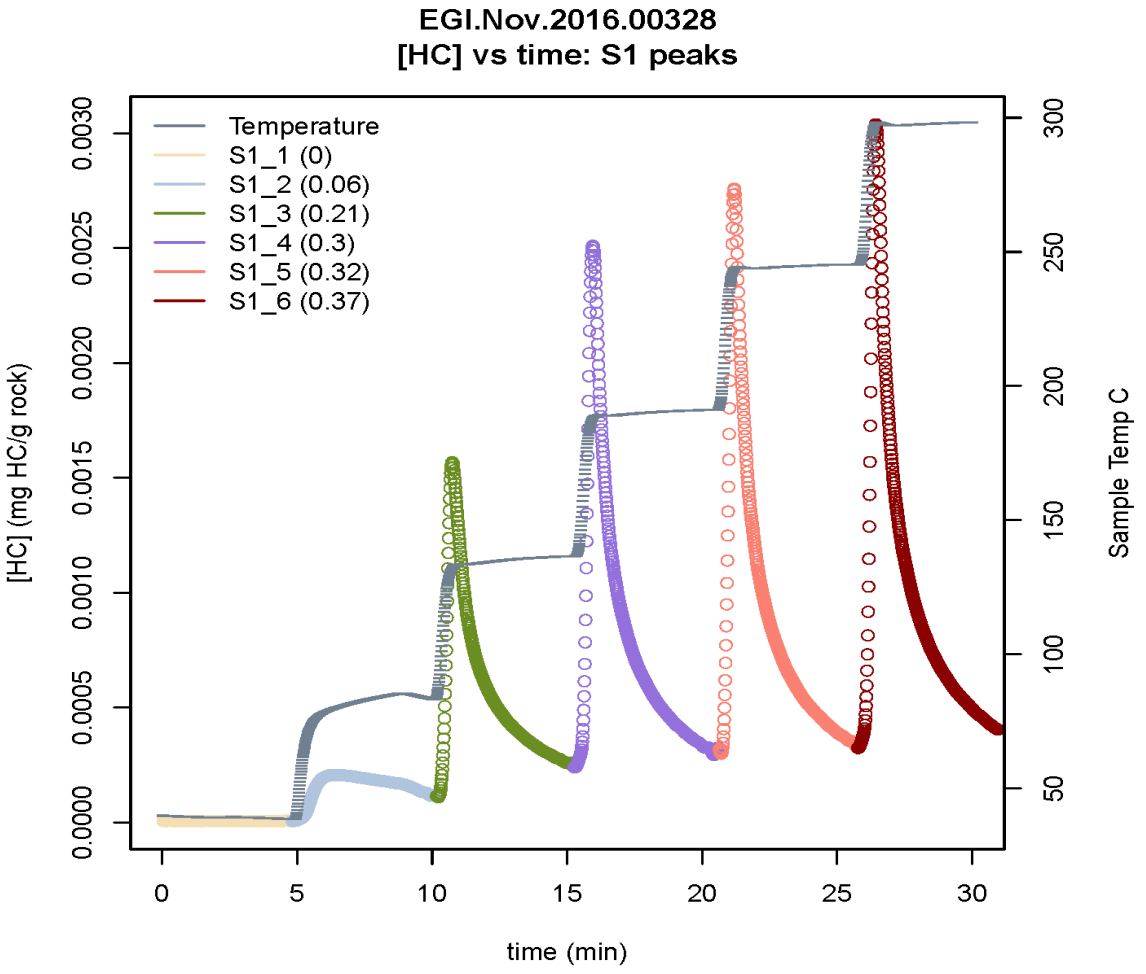

Figure G.1: S1 peaks following the general trend of gradually increasing signals for samples in the low maturity fluid window, the highest peak, S1_6 at 0.37mgHC/grock

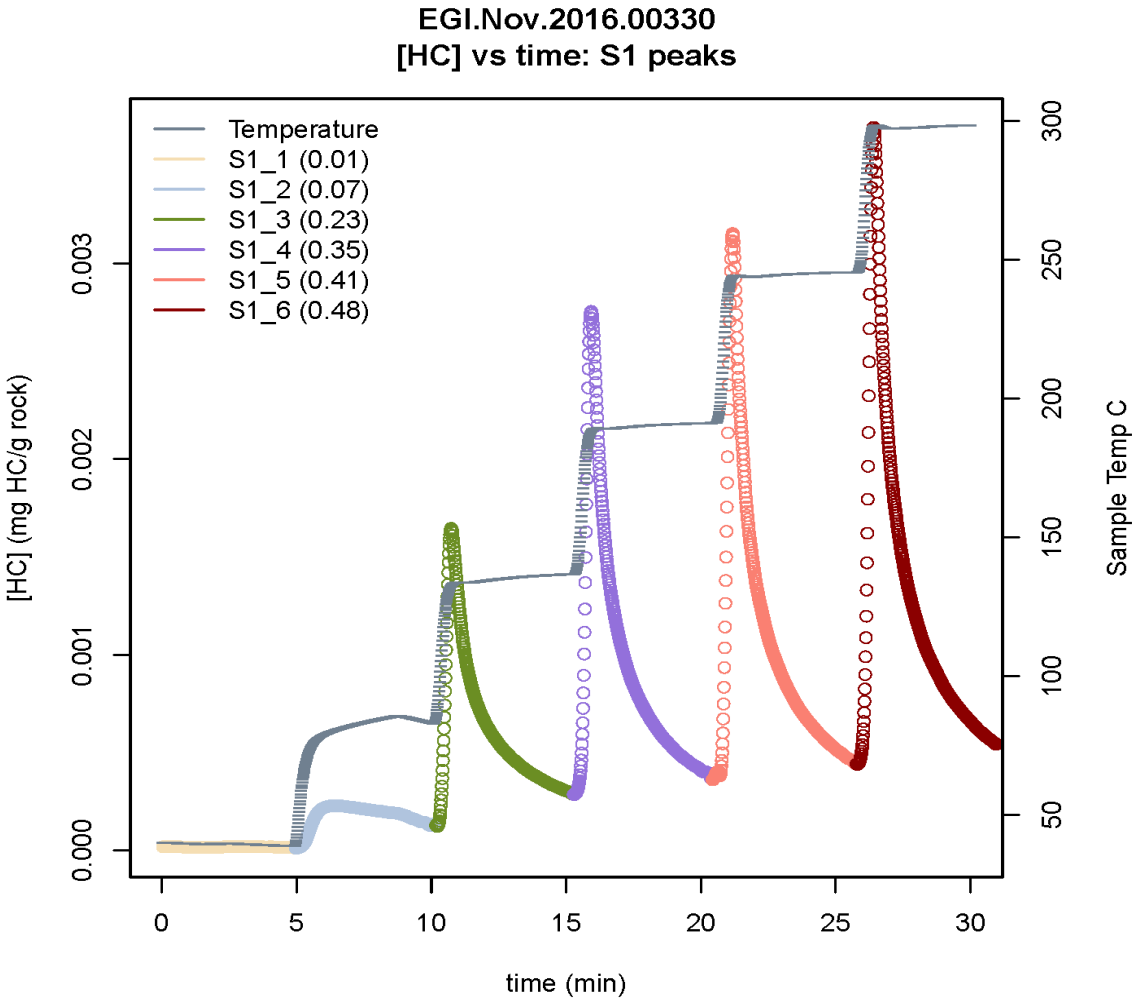

Figure G.2: S1 peaks following the general trend of gradually increasing signals for samples in the low maturity fluid window, with the highest peak, S1_6 generated at 0.48 mgHC/g rock.

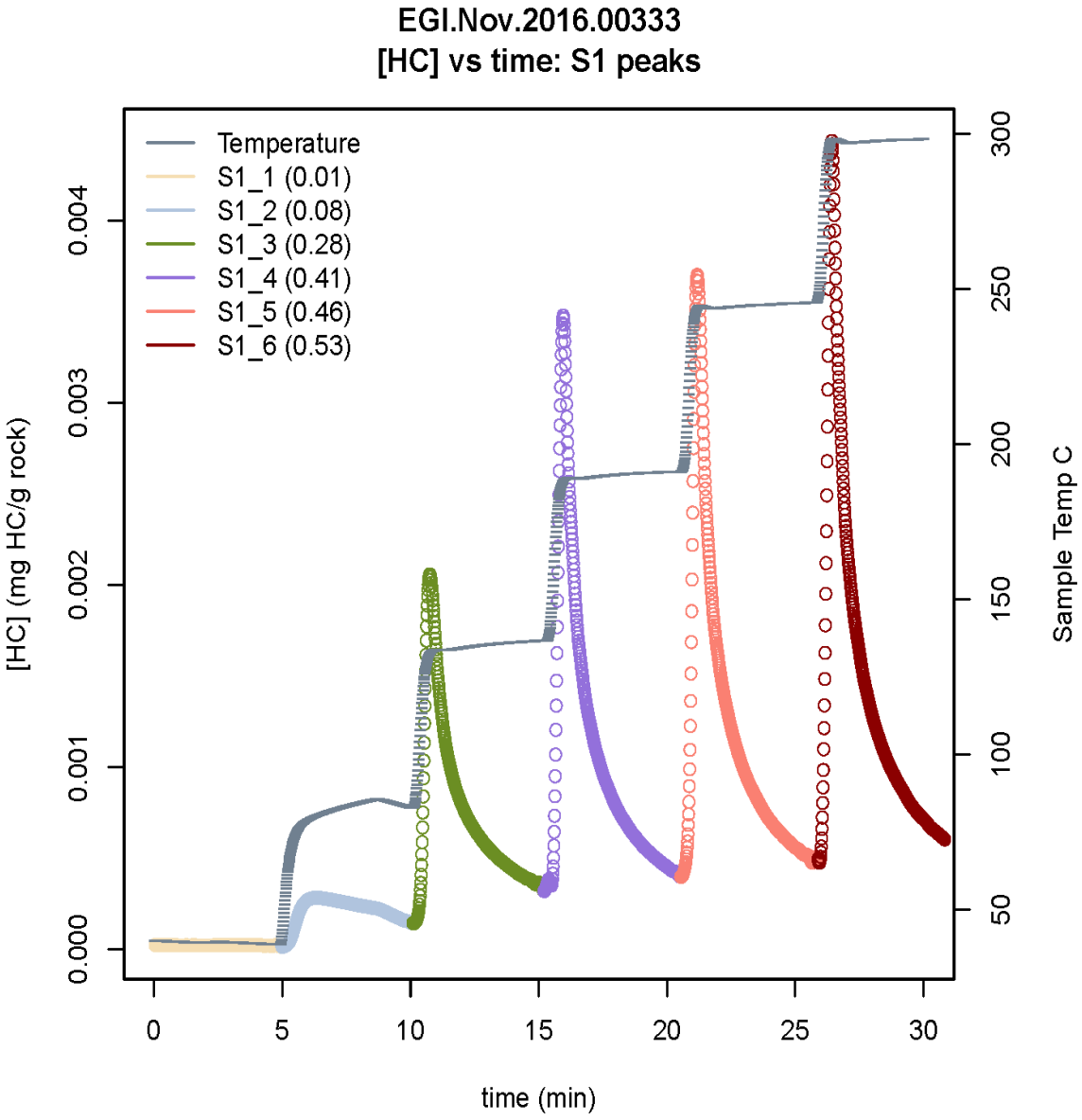

Figure G.3: S1 peaks following the general trend of gradually increasing signals for samples in the low maturity fluid window, with the highest peak, S1_6 generated at 0.53 mgHC/g rock.

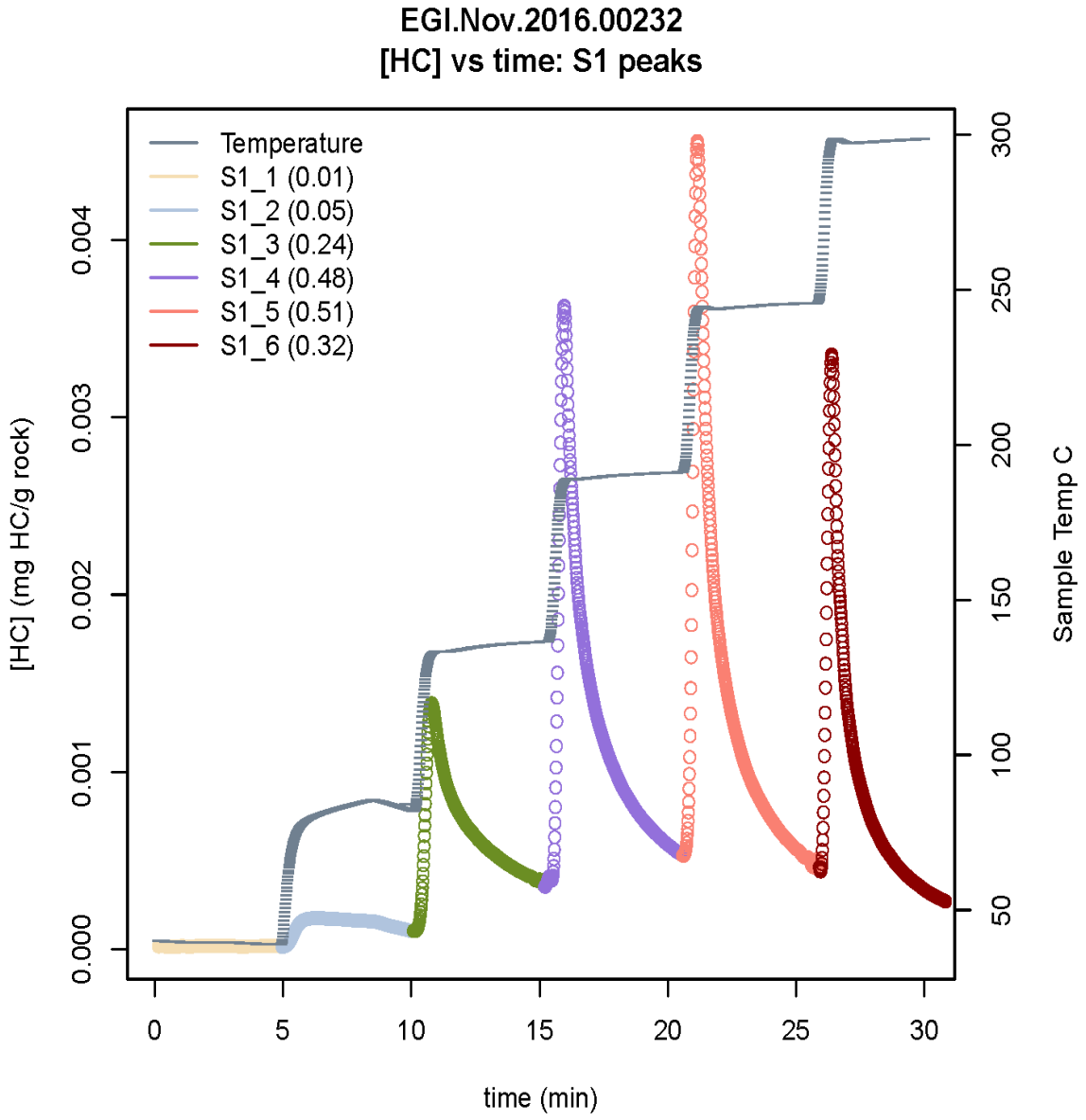

Figure G.4: A sample in the condensate maturity fluid window. In general, these samples have higher S1_4 and S1_5 peaks, but lower S_6 peaks. However, the higher of the S1_4 and S1_5 peaks do vary by sample, and do not follow any distinct pattern. In this figure, S1_5 is highest at 0.51 mgHC/g of rock.

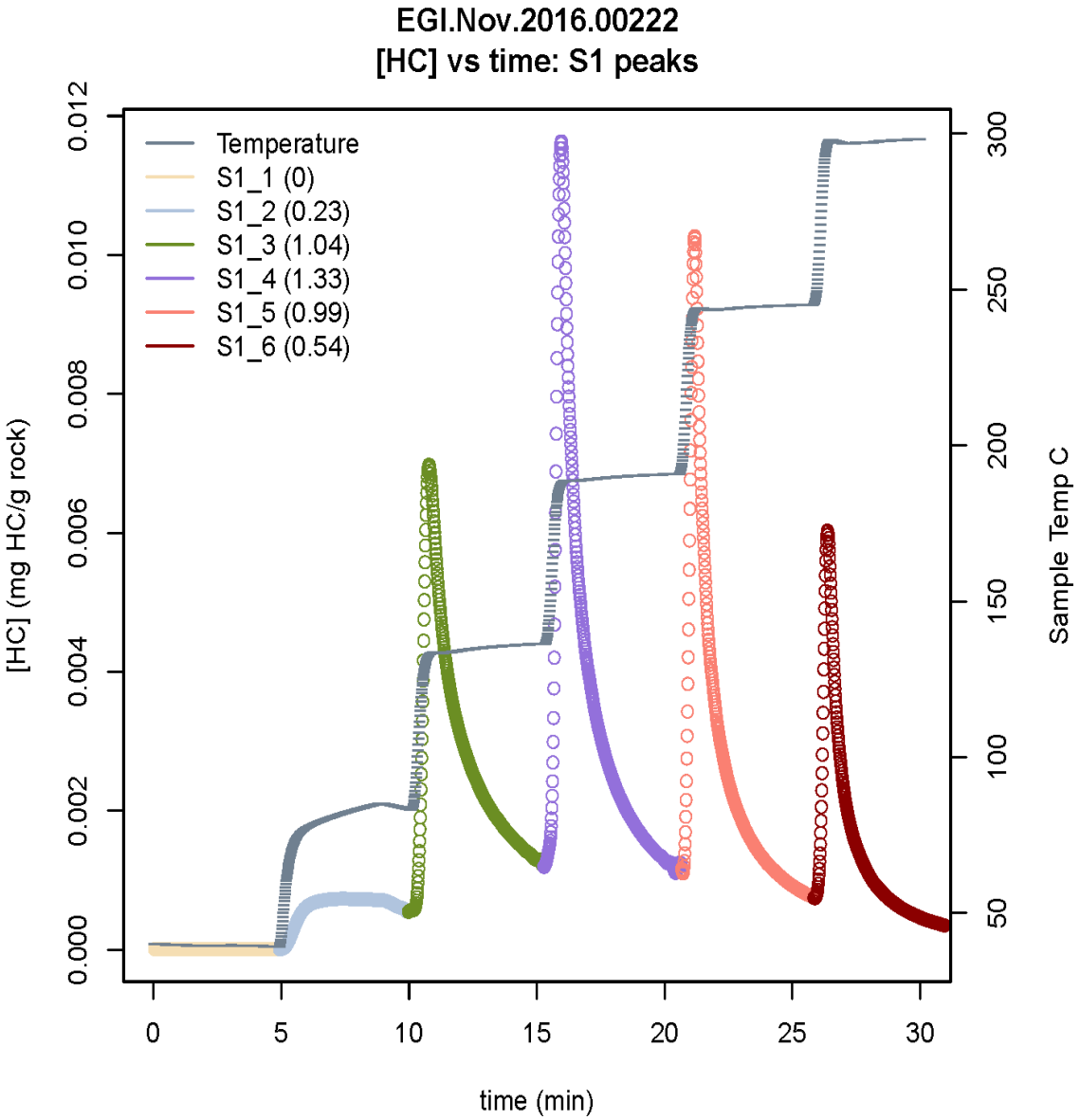

Figure G.5: A sample in the condensate maturity fluid window. In general, these samples have higher S1_4 and S1_5 peaks, but lower S_6 peaks. However, the higher of the S1_4 and S1_5 peaks do vary by sample, and do not follow any distinct pattern. In this figure, S1_4 is highest at 1.33 mgHC/g of rock.

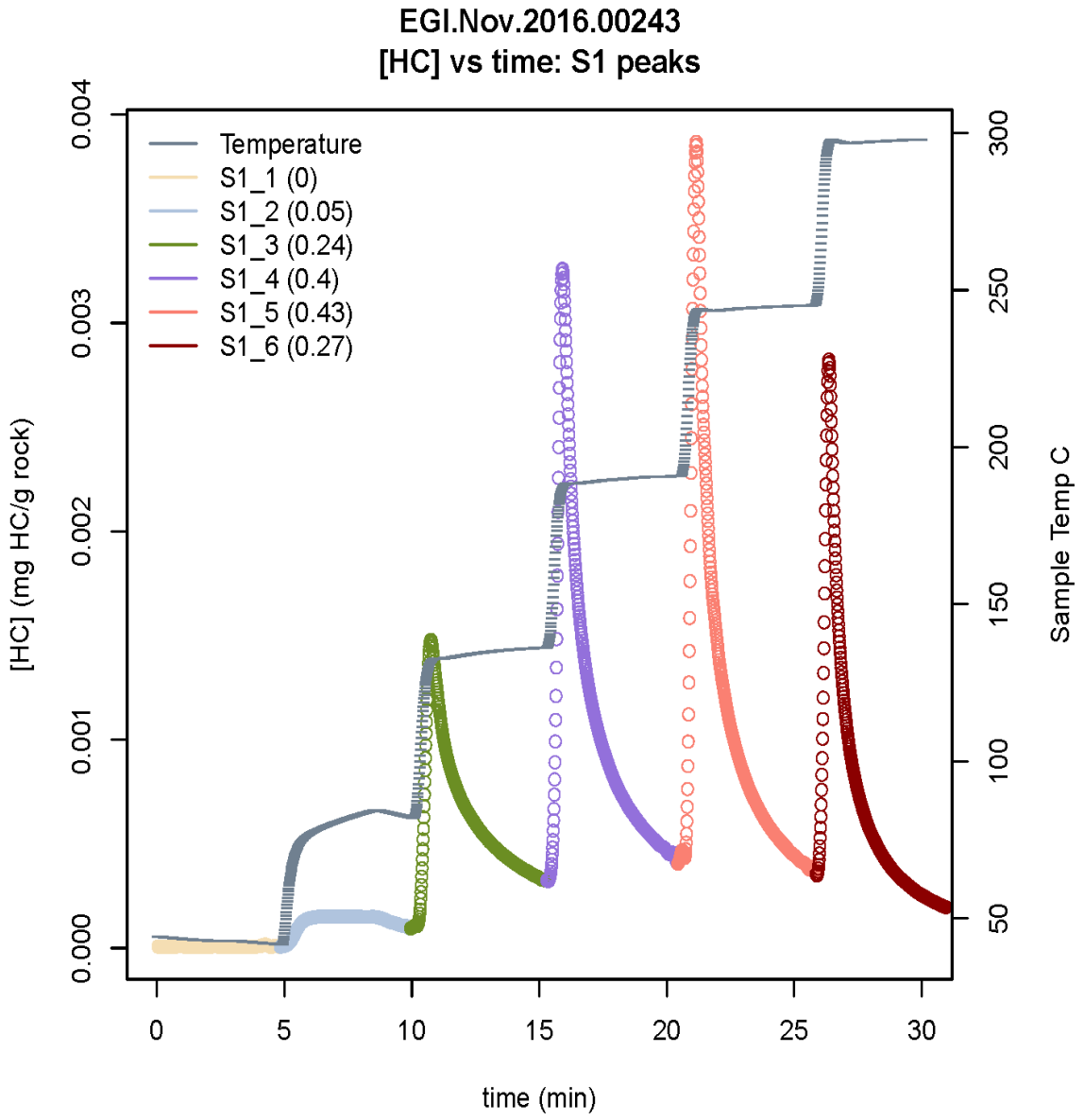

Figure G.6: A sample in the condensate maturity fluid window. In general, these samples have higher S1_4 and S1_5 peaks, but lower S_6 peaks. However, the higher of the S1_4 and S1_5 peaks do vary by sample, and do not follow any distinct pattern. In this figure, S1_5 is highest at 0.43 mgHC/g of rock.

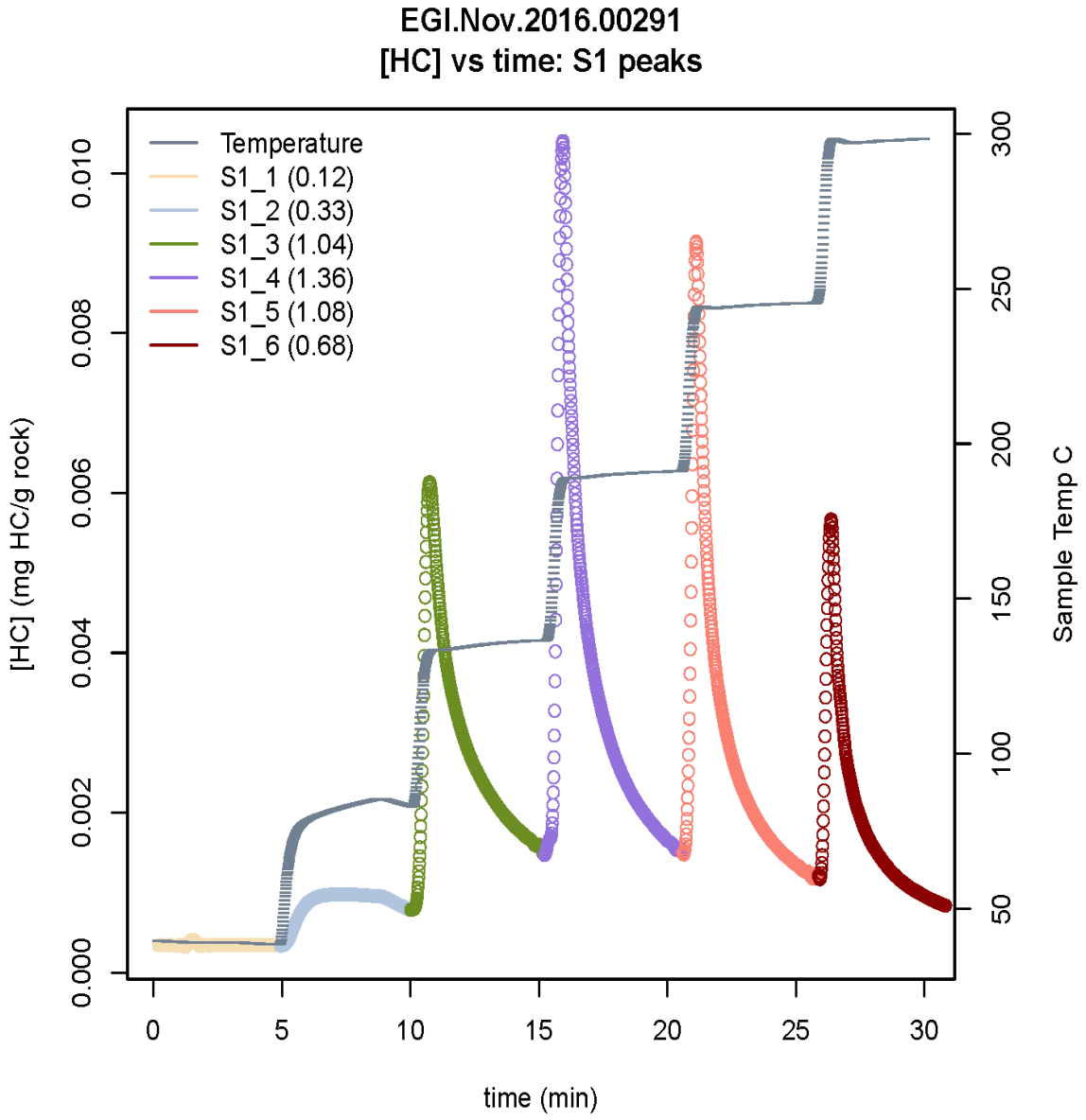

Figure G.7: A sample in the condensate maturity fluid window. In general, these samples have higher S1_4 and S1_5 peaks, but lower S_6 peaks. However, the higher of the S1_4 and S1_5 peaks do vary by sample, and do not follow any distinct pattern. In this figure, S1_4 is highest at 1.36 mgHC/g of rock.

REFERENCES

Beti, D. R. 2016. Determination of American Petroleum Institute Gravity of Petroleum in the Rock Using Pyrolysis. MS thesis, University of Utah, Salt Lake City, Utah (May 2016).

Dembicki Jr., H., Horsfield, B., and Ho, T. 1983. Source Rock Evaluation by Pyrolysis-Gas Chromatography. ***The American Association of Petroleum Geologists* 67** (7): 1094-1103. http://archives.datapages.com/data/bulletns/1982-83/data/pg/0067/0007/1050/1094.htm.

Dembicki, H., 2009. Three Common Source Rock Evaluation Errors Made by Geologists During Prospect or Play Appraisals. ***AAPG Bulletin* 93** (3): 341-356. http://archives.datapages.com/data/bulletns/2009/03mar/BLTN08076/BLTN08076.htm.

DrillingInfo. 2017. *DrillingInfo State of Ohio Historical Production Database*, http://www.drillinginfo.com/frameInfo.jsp (accessed 23 February 2017).

Espitalie, J., Deroo, G., and Marquis, F. 1985. La Pyrolyse Rock-Eval et ses Applications. ***Revue de l'Institut Francais du Petrole 40*** (5): 563-579. http://dx.doi.org/10.2516/ogst:1985035.

Espitalié J., Deroo G., and Marquis F. 1985. La pyrolyse RockEval et ses Applications. Deuxième Partie. ***Revue de l'Institut Français du Pétrole* 40** (6): 755-784. http://dx.doi.org/10.2516/ogst:1985045.

Espitalié J., Deroo G., and Marquis F. 1986. La Pyrolyse RockEval et ses Applications.Troisième Partie. ***Revue de l'Institut Français du Pétrole* 41** (1): 73-89. http://dx.doi.org/10.2516/ogst:1986003.

Espitalié J., Laporte J.L., Madec M., et al. 1977. Méthode Rapide de Caractérisation Des Roches Mères, de Leur Potential Pétrolier et de Leur Degré D'evolution. ***Revue de l'Institut français du pétrole* 32** (1): 23–42. http://dx.doi.org/10.2516/ogst:1977002.

Jarvie, Daniel M. 2015. Advances in Organic Geochemistry. Van Tuyl Lecture presented 29 October 2015, School of Mines, Golden, Colorado.

Jarvie, Daniel M. 2015. Comparison of Source/Reservoir Rock to Produced Petroleum Composition. ***AAPG Datapages/Search and Discovery Article #90216***, http://www.searchanddiscovery.com/abstracts/html/2015/90216ace/abstracts/2091897.html (accessed 14 January 2016).

Maende, A. and Weldon, D. 2016. The Theory, Measurements, Interpretation and Applications of Pyrolysis & TOC Data. www.wildcattechnologies.com (accessed 17 August 2016).

Murphy, E., Warner, M. and Sarmah, B. 2013. A Workflow to Evaluate Porosity, Mineralogy, and TOC in the Utica-Point Pleasant Shale Play. SPE -165682-MS. https://www.onepetro.org/conference-paper/SPE-165682-MS.

ODNR Division of Oil & Gas Resources. 2017. Oil & Gas Well Production. http://oilandgas.ohiodnr.gov/production#ARCH1 (accessed 4 January 2017).

Ohio Department of Natural Resources. 2017. Calculated %Ro Average per Well of the Upper Ordovician Shale Interval in Ohio, https://geosurvey.ohiodnr.gov/portals/geosurvey/Energy/Utica/Ordov-Shale_Ro-Average_03-2013.pdf (downloaded 15 January 2017).

Ohio Department of Natural Resources. 2017. Horizontal Utica - Pt Pleasant Well Activity in Ohio, http://oilandgas.ohiodnr.gov/Portals/oilgas/pdf/activity_maps/HorizontalWells_MonthlyUticaPagesize_12032016.pdf (downloaded 4 January 2017).

Ruble, Tim, Drozd, Richard J. and Heck, William A. 2017. Practical Geochemical Methods to Assess Unconventional Reservoirs: A Case Study from the Permian Basin, Texas, http://www.wtgs.org/media/files/None/2012_Ruble_WFTL_WTGS_Presentation.pdf (downloaded 4 January 2017).

Wickstrom, L. H., Riley, R. and Erenpreiss, M. 2012. Geologic Overview and Activity Update for the Utica-Point Pleasant Shale Play in Ohio. ***AAPG Datapages/Search and Discovery Article #10409***, http://www.searchanddiscovery.com/pdfz/documents/2012/10409wickstrom/ndx_wickstrom.pdf.html (downloaded 14 January 2016).

Wickstrom, L. and Shumway, M. 2014. A First Look at Production and Completion Data from the Utica-Point Pleasant Play or...Having Fun with Numbers. ***AAPG Datapages/Search and Discovery Article #10661***, http://www.searchanddiscovery.com/documents/2014/10661wickstrom/ndx_wickstrom.pdf (downloaded 14 January 2016).

Wickstrom, L., Erenpreiss, M., Riley, R., et al. 2012. Geology and Activity Update of the Ohio Utica-Point Pleasant Play, https://geosurvey.ohiodnr.gov/portals/geosurvey/energy/Utica/Utica-PointPleasantPlay.pdf (downloaded 24 August 2016).

Wildcat Technologies. 2016. HAWK Workstation Manual, https://www.wildcattechnologies.com/products/hawk (accessed 20 October 2016).

Wildcat Technologies. 2016. Hawk: Our Flagship Instrument, https://www.wildcattechnologies.com/products (accessed 20 October 2016).

Wright, M. C., Court, R. W., Kafantaris, F., et al. 2015. A new rapid method for shale oil and shale gas assessment, http://www.sciencedirect.com/science/article/pii/S0016236115002513 (accessed 4 February 2017).